Measurement of the Induced $\Lambda(1116)$ Polarization in K^+ Electroproduction at CLAS

M. Gabrielyan[1], B. Raue[1], D.S. Carman[2], K. Park[2]

1. Florida International University
2. Jefferson Lab

CIPANP 2012

6/1/2012

FLORIDA INTERNATIONAL UNIVERSITY
Miami's public research university

Jefferson Lab

Outline

- Motivation. Why study ground state hyperon electroproduction?
- CLAS Detector
- PID
- Polarization extraction
- Analysis results
- Summary

Motivation

This study is *part* of a larger program that has a goal of measuring as many observables as possible for *KY* electroproduction.

- Electroproduction allows $Q^2 \neq 0$ kinematics. Virtual photon possesses both transverse and longitudinal polarizations that allow access to interference response functions that are inaccessible through photoproduction.

- Understand which *N*'s* couple to *KY* final states.

- These data are needed in a coupled-channel analysis to identify previously unobserved *N** resonances.

- Get a better understanding of the strange-quark production process by mapping out the kinematic dependencies for these observables.

CEBAF Large Acceptance Spectrometer

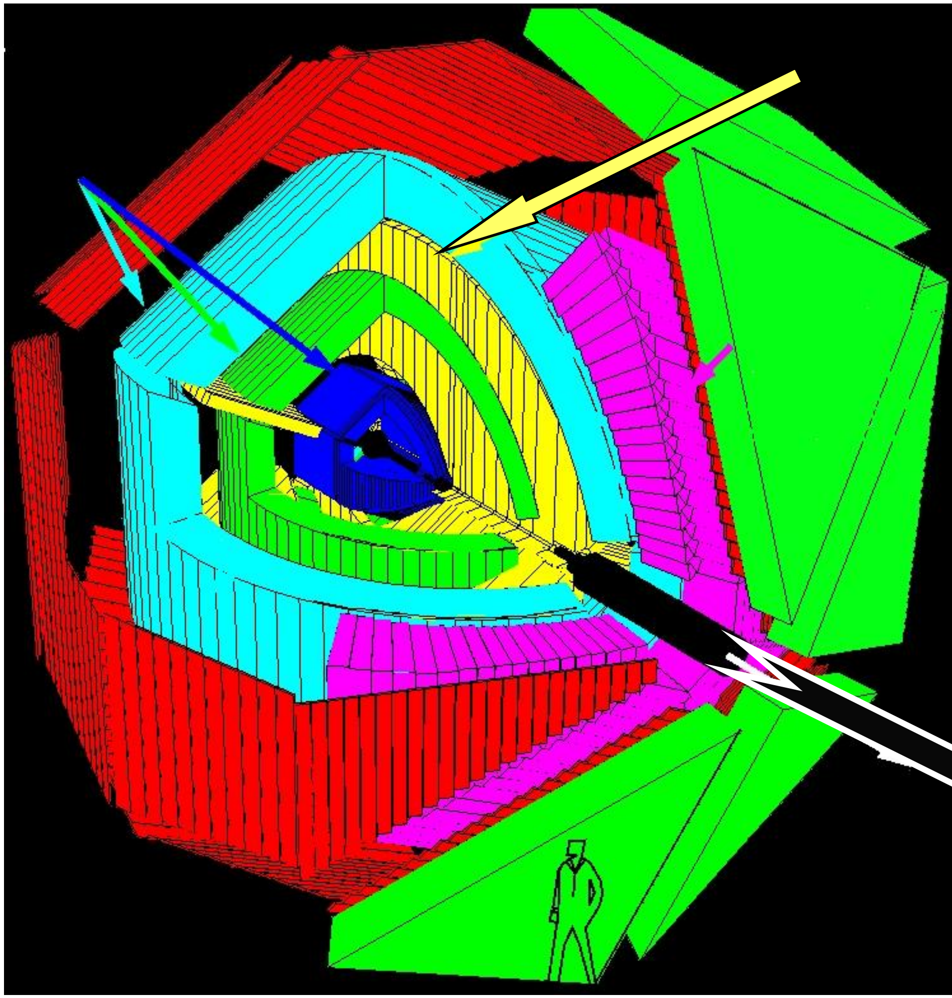

- Torroidal magnetic field in region 2

beam direction

CEBAF Large Acceptance Spectrometer

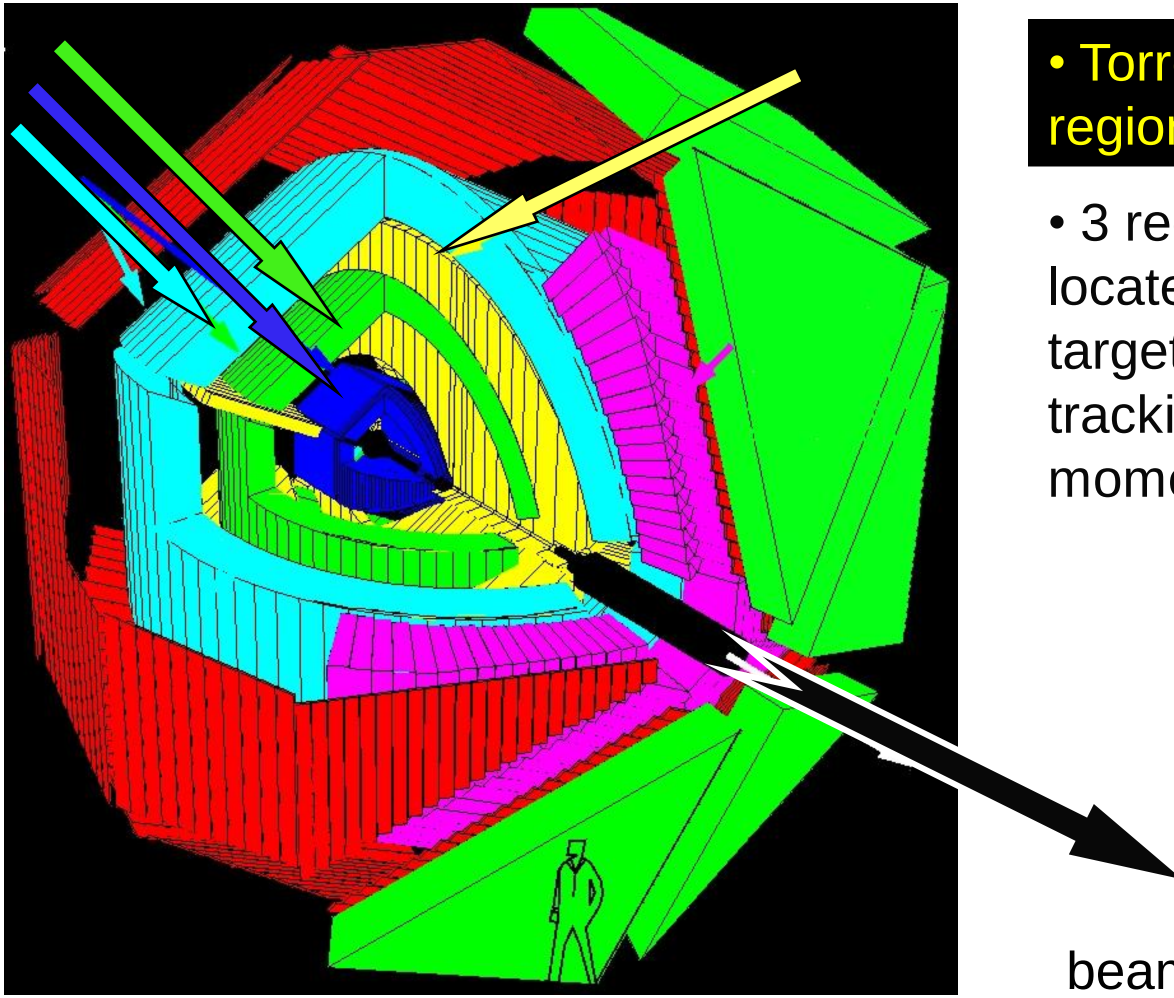

- Torroidal magnetic field in region 2

- 3 regions of drift chambers located spherically around target provide charge particle tracking for angle and momentum reconstruction.

beam direction

CEBAF Large Acceptance Spectrometer

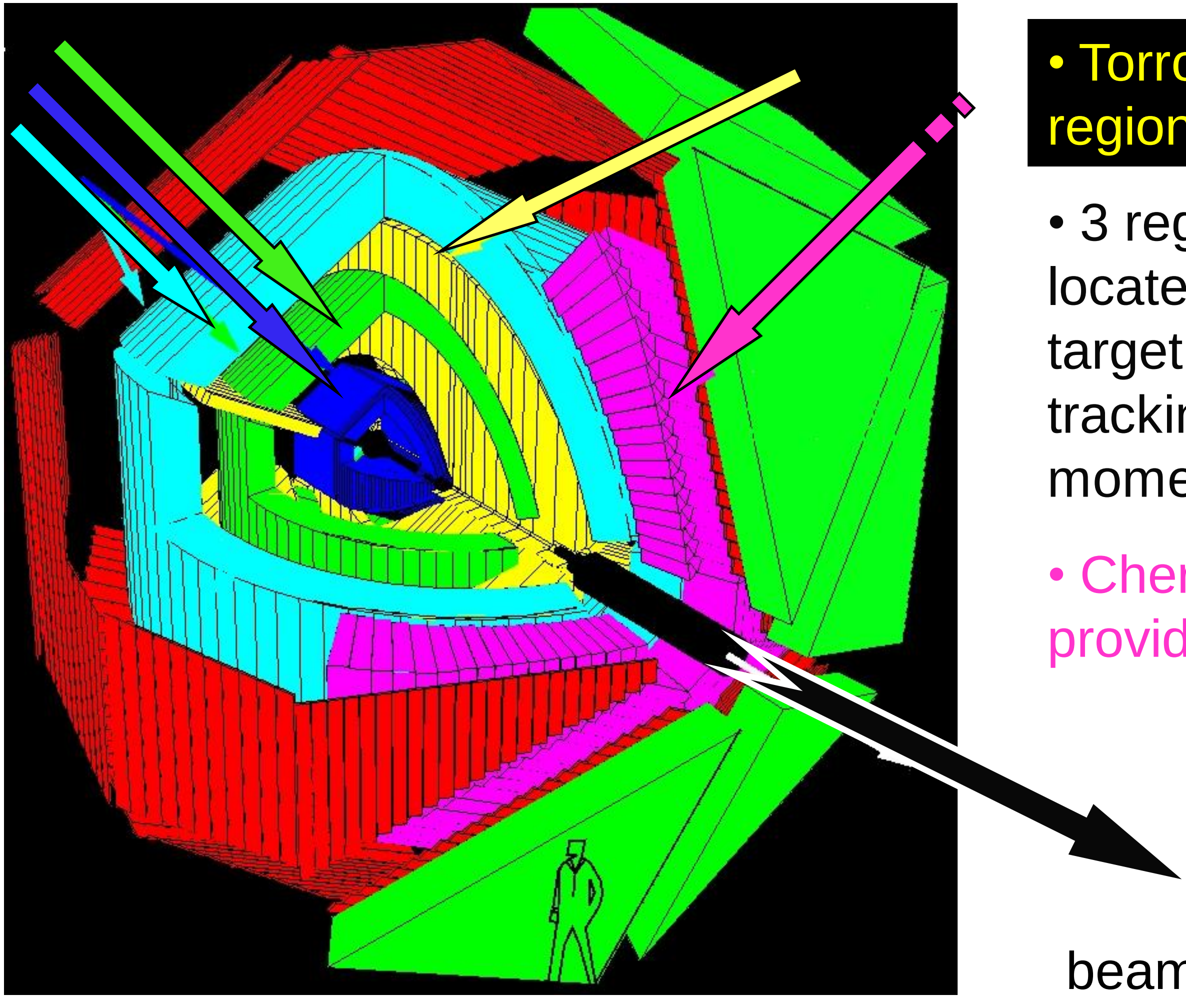

• Torroidal magnetic field in region 2

• 3 regions of drift chambers located spherically around target provide charge particle tracking for angle and momentum reconstruction.

• Cherenkov detectors provide e/π separation

beam direction

CEBAF Large Acceptance Spectrometer

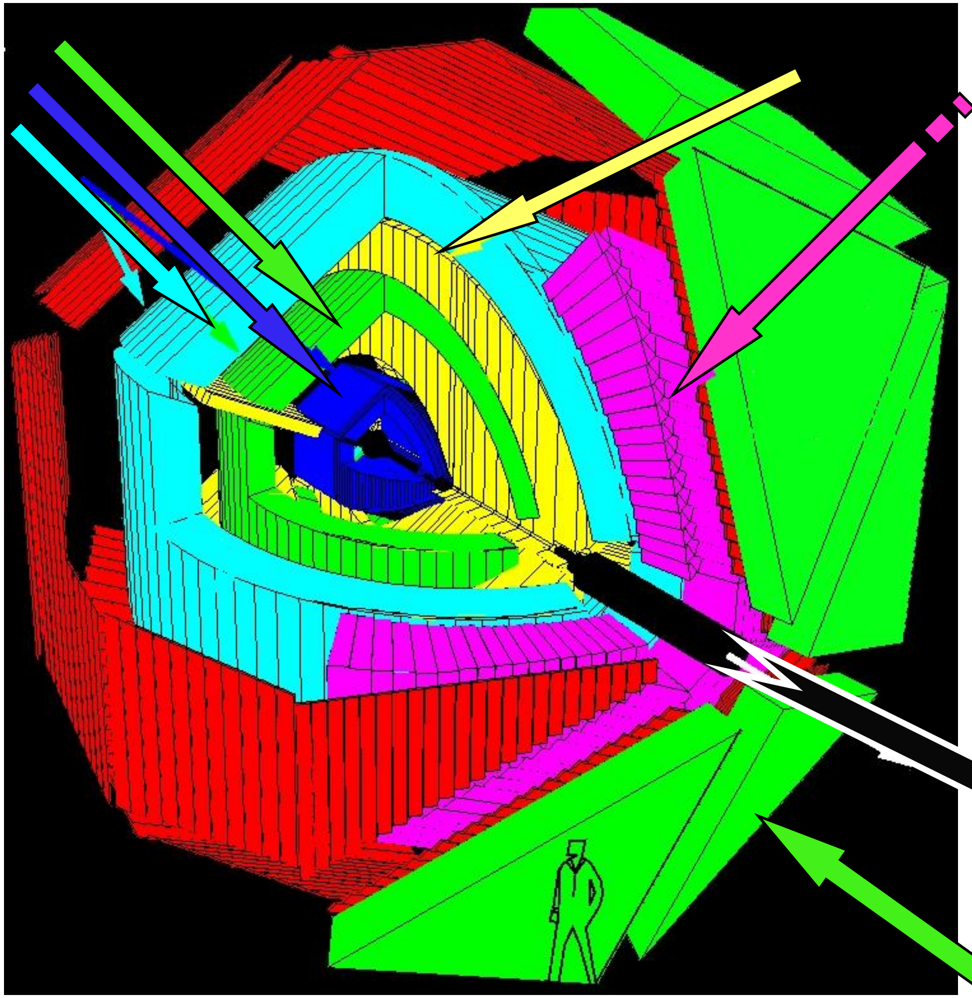

• Torroidal magnetic field in region 2

• 3 regions of drift chambers located spherically around target provide charge particle tracking for angle and momentum reconstruction.

• Cherenkov detectors provide e/π separation

• Electromagnetic calorimeter gives total energy measurement for electrons and neutrals and also e/π separation

beam direction

CEBAF Large Acceptance Spectrometer

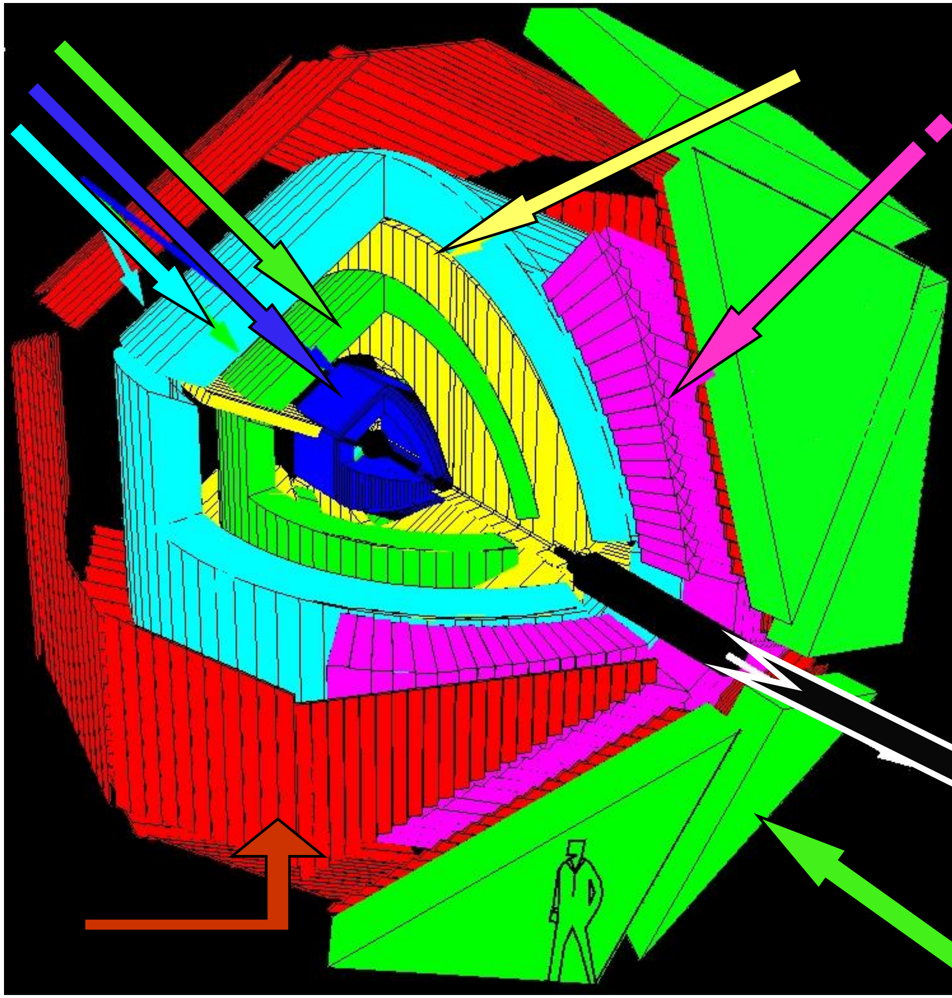

- Torroidal magnetic field in region 2

- 3 regions of drift chambers located spherically around target provide charge particle tracking for angle and momentum reconstruction.

- Cherenkov detectors provide e/π separation

- Electromagnetic calorimeter gives total energy measurement for electrons and neutrals and also e/π separation

beam direction

- Time of flight scintillators $\rightarrow \beta \rightarrow$ particle ID

Kinematics and E1F Dataset

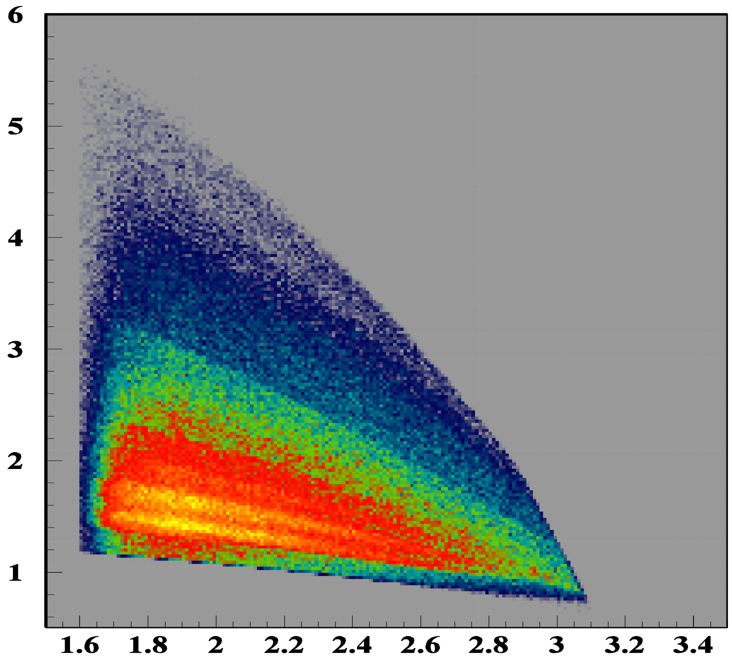

Q^2 vs W

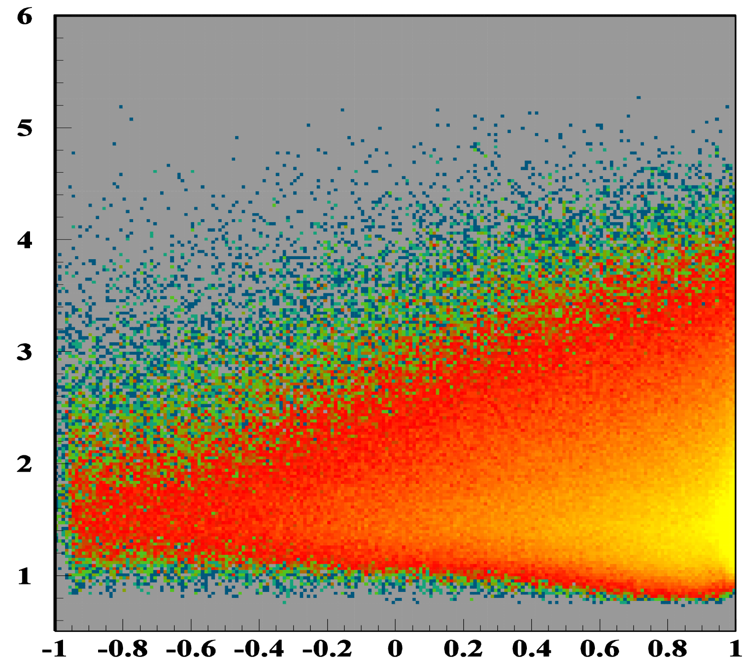

Q^2 vs $\cos(\theta_K^{CM})$

- Beam energy = 5.5 GeV
- Unpolarized Target
- Torus current = 2250 A
- 5B triggers, 213000 Λ's

- $0.8 < Q^2 < 3.5$ GeV^2
- $1.6 < W < 2.8$ GeV
- $-1.0 < \cos(\vartheta_K^{CM}) < 1.0$

Particle Identification

Electrons:

- Coincidence between CC and EC in the same sector.
- Negatively charged track in DC that matches in time with TOF.
- Momentum corrections applied to correct for DC misalignments and inaccuracies in the magnetic field map.

Hadrons: Time difference (Δt) between the measured time and the computed time for a given hadron species (π^+, K^+, p).

Minimum *Δt identifies the hadron.*

Hadron Identification

Minimum *Δt* identifies the hadron.

After Λ and π missing mass cuts

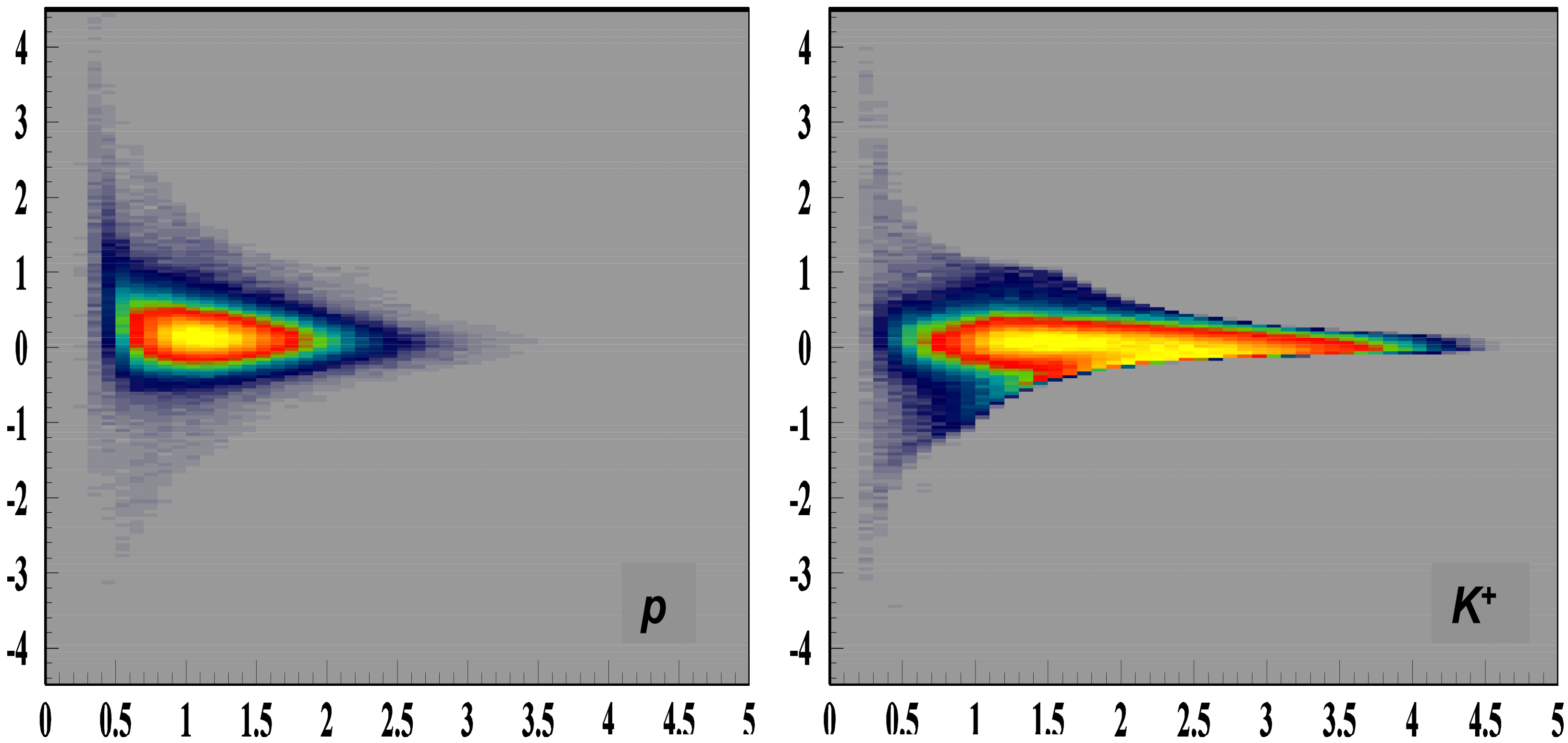

Minimum Δt vs p

Hadron Identification

Minimum *Δt* identifies the hadron.

After Λ and π missing mass cuts

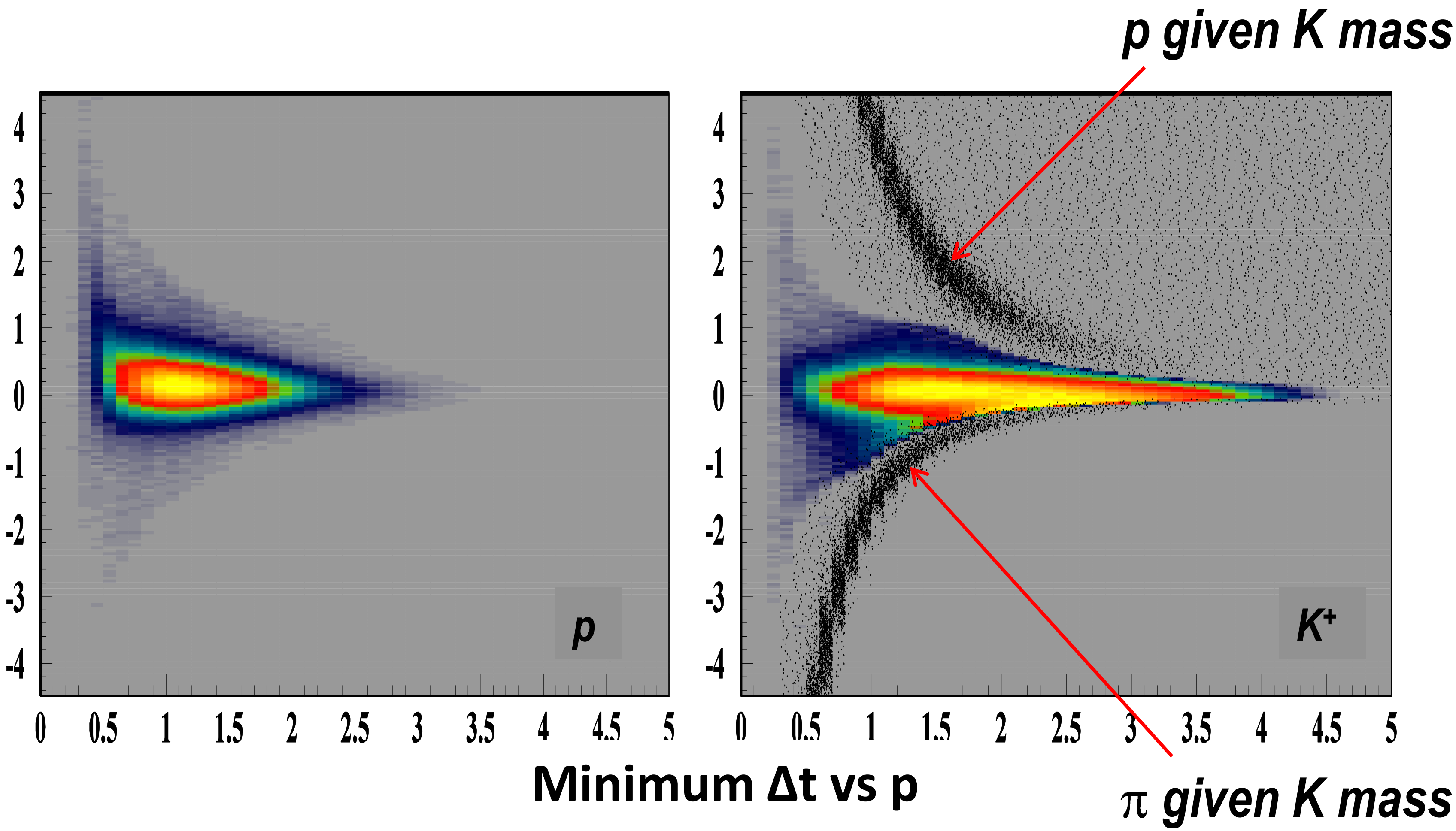

Λ Identification

- Reconstructed missing mass for $e+p \rightarrow e'K^+(X)$
- For recoil polarization observables $e+p \rightarrow e'K^+p(\pi^-)$ include π^- missing-mass cut

$$E_1 + E_2 = E_3 + E_4 + E_X$$

$$\vec{p}_1 + \vec{p}_2 = \vec{p}_3 + \vec{p}_4 + \vec{p}_X$$

$$M_X^{\ 2} = E_X^{\ 2} - p_X^{\ 2}$$

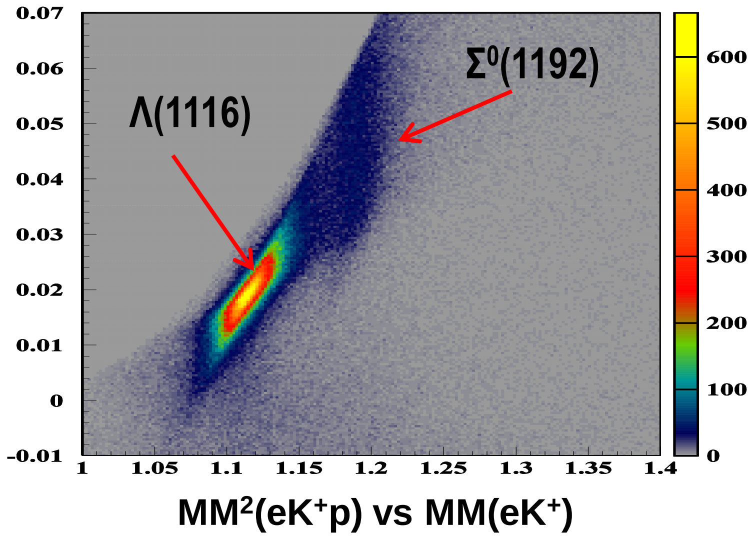

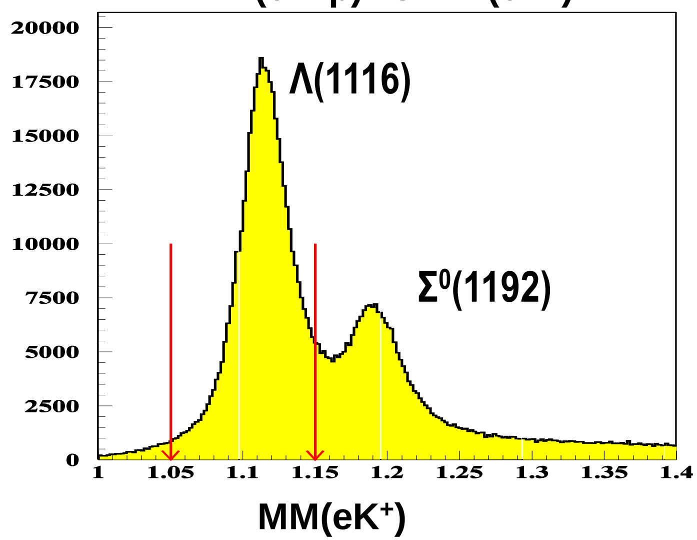

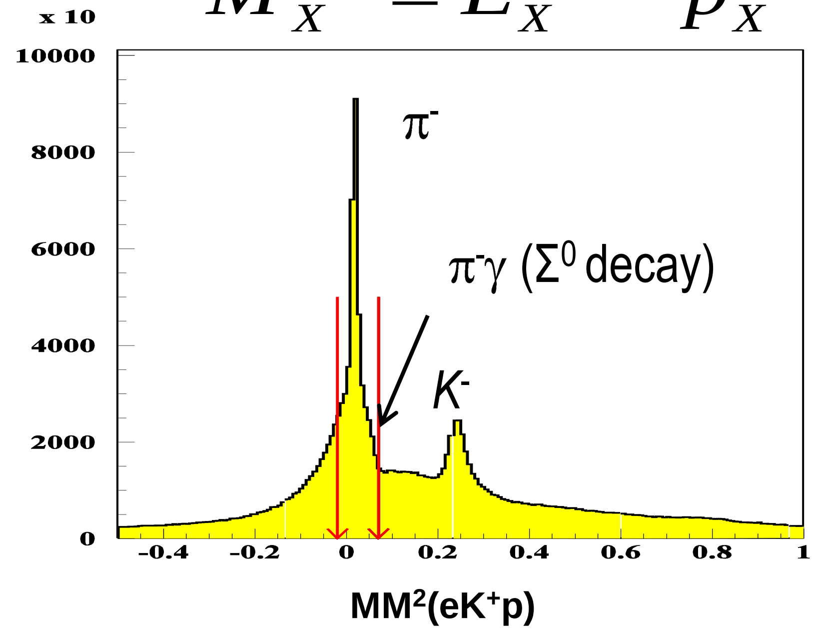

Background in the hyperon missing mass spectrum is dominated by π's misidentified as K⁺.

Cross Section for Electroproduction

$$\frac{d\sigma}{dE' d\Omega_e d\Omega_K^*} = \Gamma \frac{d\sigma_v}{d\Omega_K^*}$$

Polarized beam & recoil Λ, unpolarized target.

$$\frac{d\sigma_v}{d\Omega_K^*} = \sigma_0 (1 + hA_{LT'} + P_{x'} \hat{x}' \cdot S' + P_{y'} \hat{y}' \cdot S' + P_{z'} \hat{z}' \cdot S')$$

Where:

$$A_{LT'} = \frac{K_f}{\sigma_0} \sqrt{2\varepsilon_L (1-\varepsilon)} R_{LT'}^{00} \sin\Phi$$

$$P_{i'} = P_{i'}^0 + hP_{i'}^{'}$$

Transferred polarization

Induced polarization

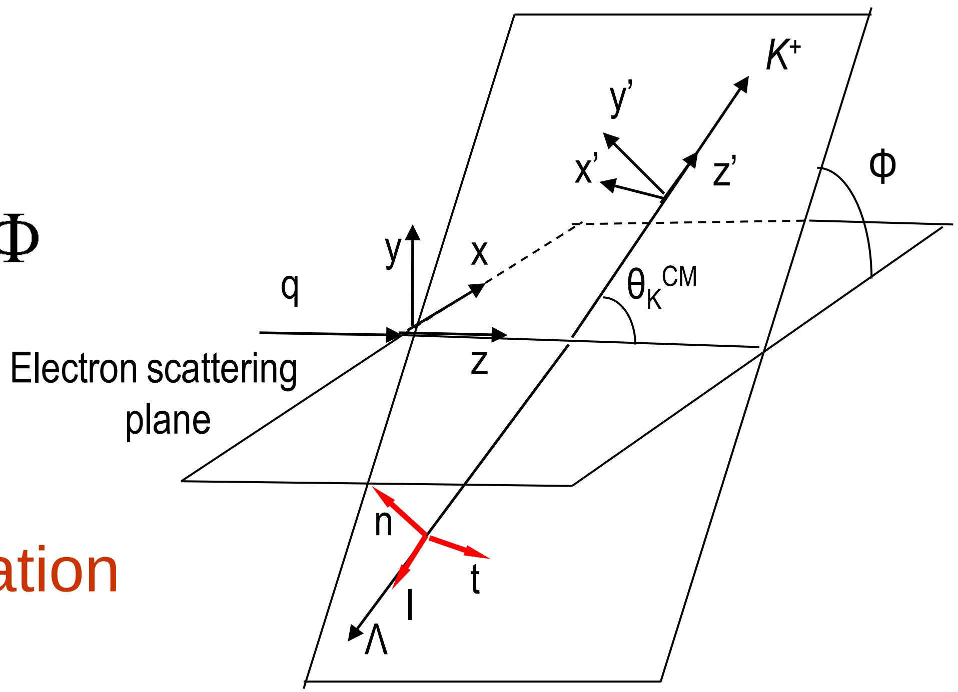

Λ Polarization Extraction

Parity non-conservation in weak decay allows to extract recoil polarization from *p* angular distribution in Λ rest frame.

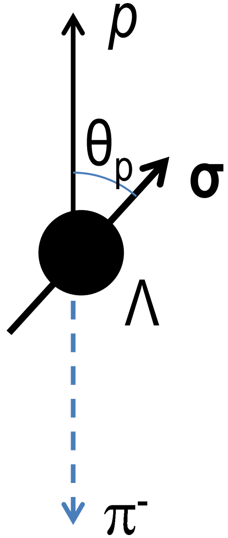

$$I(\theta_p) = 1 - \alpha \cos\theta_p$$

$$\alpha = 0.642 \pm 0.013$$

$$\vec{n} = \frac{\vec{p}_\Lambda \times \vec{p}_K}{p_\Lambda \cdot p_K}$$

$$P_\Lambda = \frac{2}{\alpha} \cdot \frac{N_F - N_B}{N_F + N_B}$$

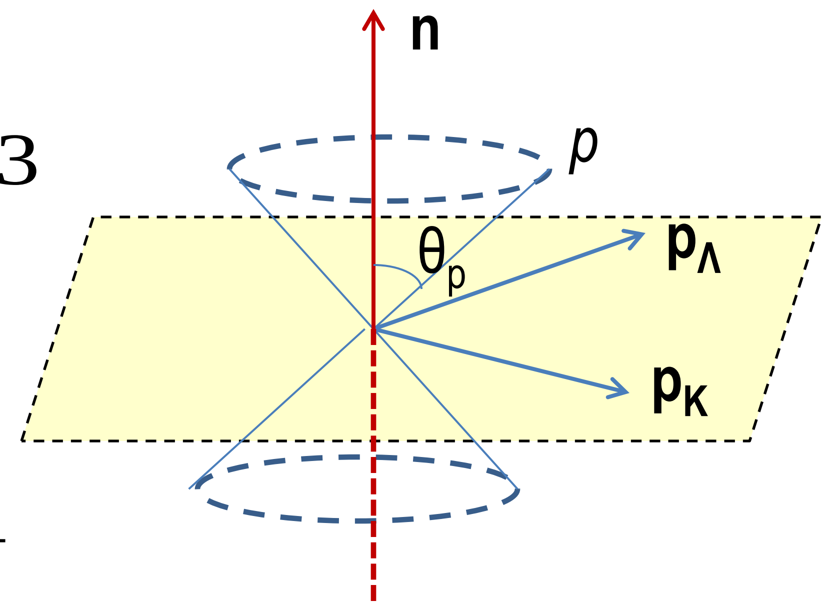

Here N_F and N_B are the acceptance corrected *p* yields above and below the K^+ Λ production plane.

After *Φ* integration only P_N component survives for induced polarization (P_L, P_T = 0).

Carman et al., PRC 79 065205 (2009)

Acceptance Corrections

FSGen: Phase space generator with modified t-slope: t-slope=0.3 GeV^{-2}

Acceptance corrections are applied to background subtracted yields.

$$f^{\pm}_{acc} = N^{\pm}_{det} / N^{\pm}_{thrown}$$

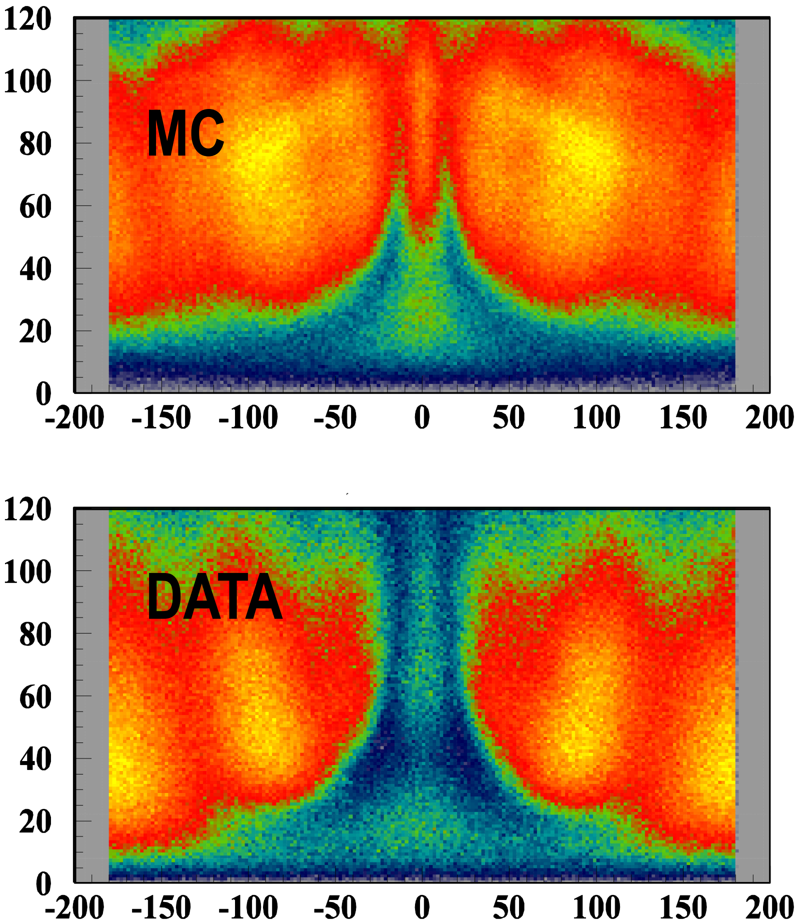

Θ_K vs φ_K CM

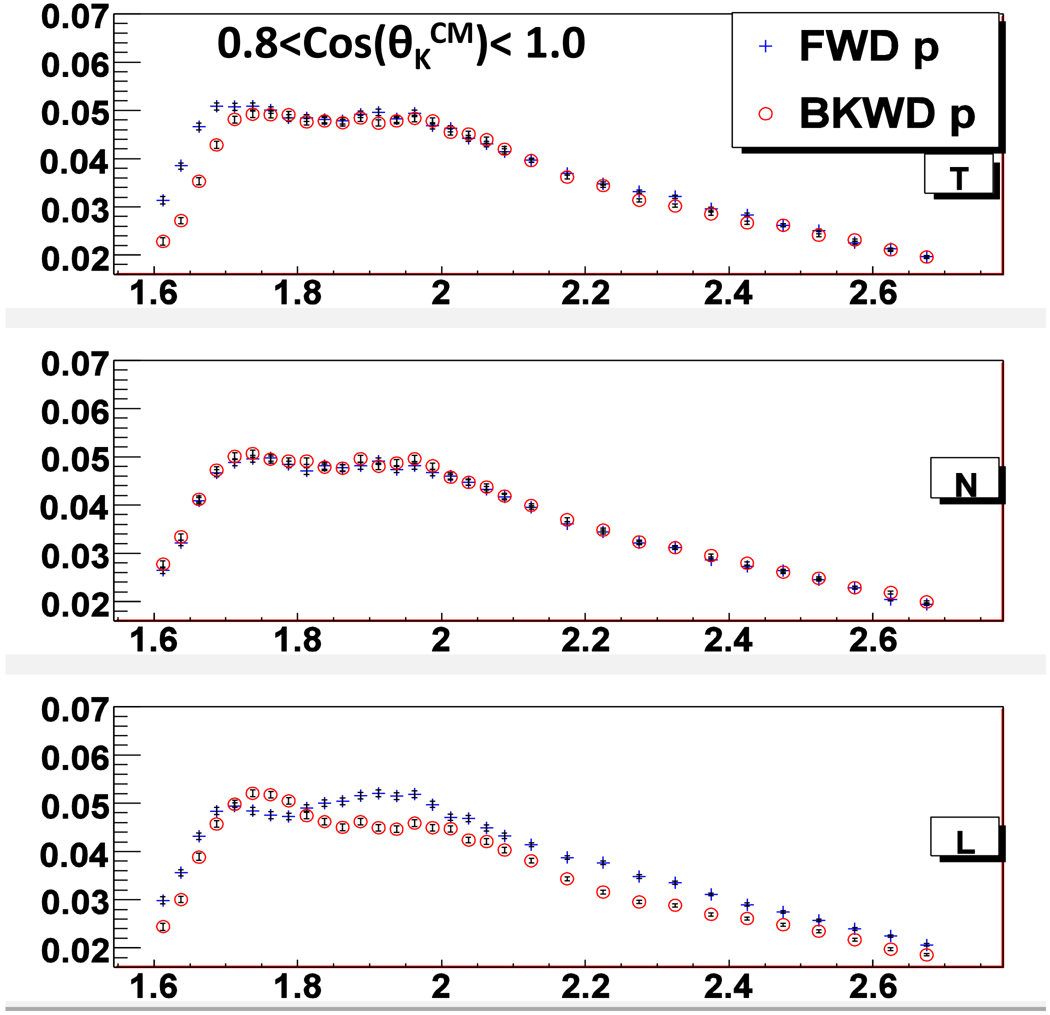

f_{acc} vs W (GeV)

Background Subtraction

The fit function form is motivated by the Λ and Σ Monte Carlo templates that are matched to data.

- $f_\Lambda = G_\Lambda + L_\Lambda^L + L_\Lambda^R$
- $f_\Sigma = G_\Sigma + L_\Sigma^L + L_\Sigma^R$
- $f_{BKG} = A*(bkg\_temp)$
- $f_{TOTAL} = f_\Lambda + f_\Sigma + f_{BKG}$

G_Λ = Gaussian,
L_Λ^L = Left Lorentzian,
L_Λ^R = Right Lorentzian,
A = Amplitude.

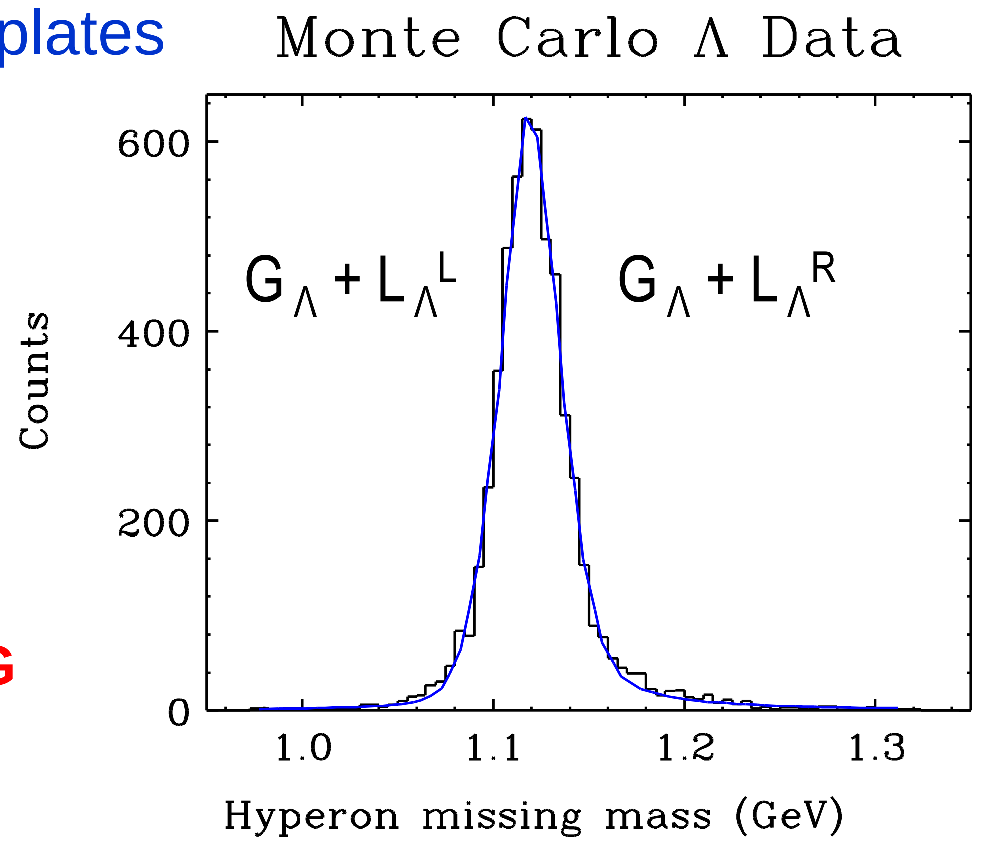

The background templates are generated from data by intentionally misidentifying pions as kaons.

Background Subtraction

1.05 < MM(eK⁺) < 1.15 GeV

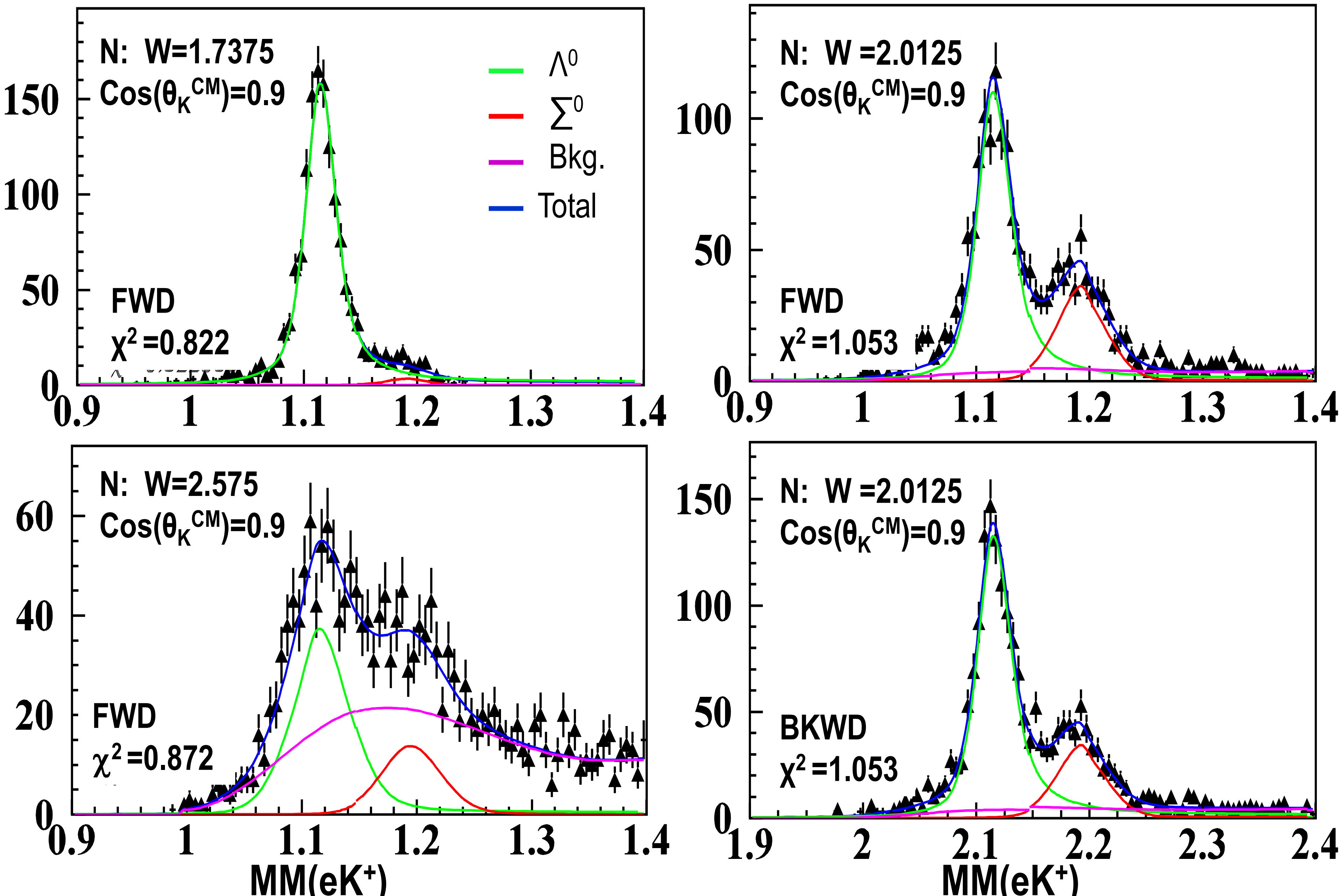

Induced Polarization P_N vs W (GeV)

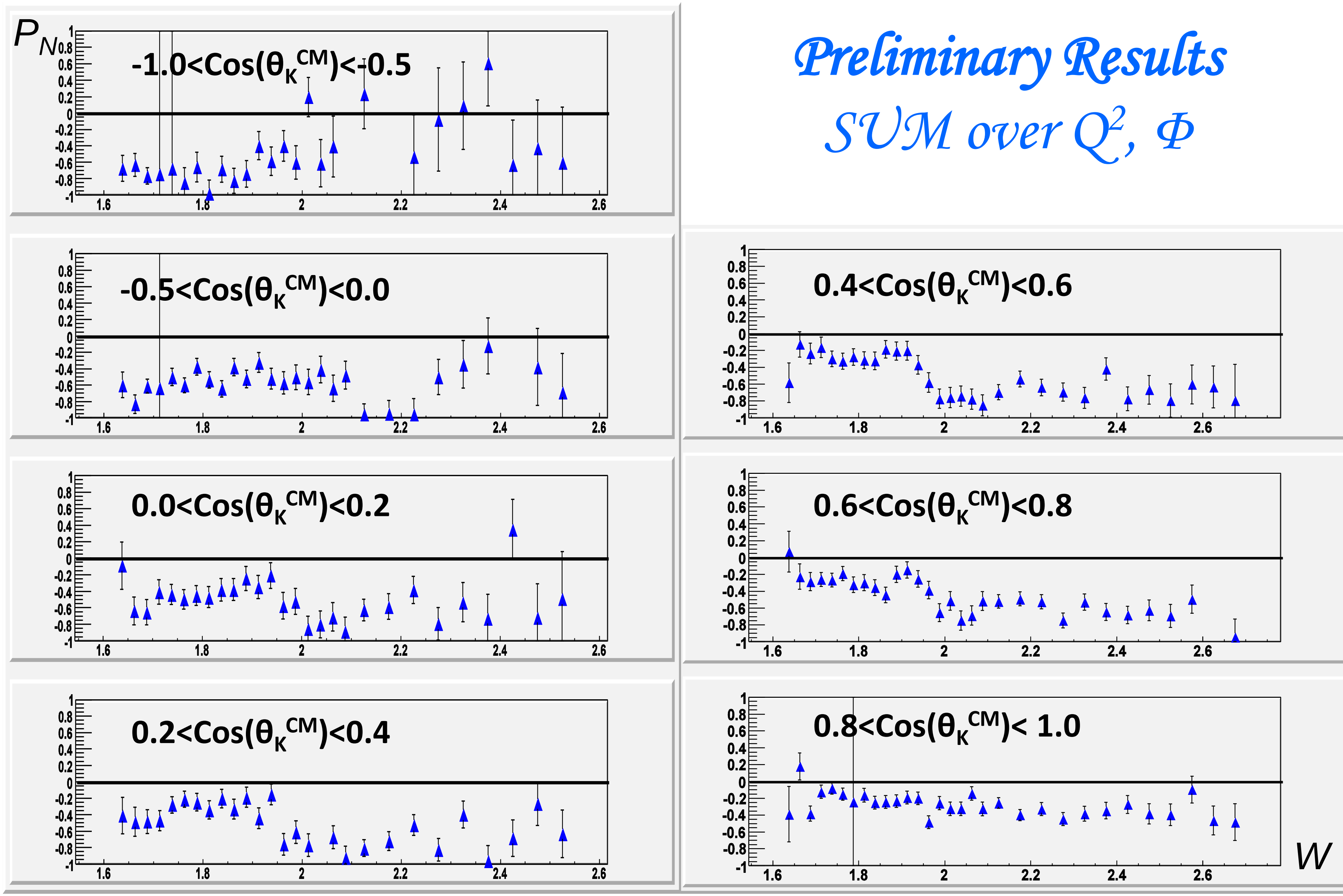

RPR Model

- Non-resonant background contributions treated as exchanges of kaonic Regge trajectories in the *t*-channel:

  K(494) and K^*(892) dominant trajectories. Both have a rotating Regge phase. This approach reduces the number of parameters.
- Included *established* *s*-channel nucleon resonances:

  S11(1650), P11(1710), P13(1720), P13(1900)
- Included *missing* resonance: D13(1900).
- Old RPR model was fit to forward angle ($\cos\theta_K^{CM} > 0$) photoproduction data (CLAS, LEPS, GRAAL) to constrain the parameters. (***T. Corthals et al., Phys. Lett. B 656 (2007))***
- RPR-2011 model was fit to the entire $\cos\theta_K^{CM}$ angular range of all recent $K^+\Lambda$ photoproduction data to constrain the parameters. Furthermore, it also includes spin-5/2 particles as described in ***T. Vrancx et al., arXiv:1105.2688.***

Induced Polarization P_N vs W (GeV)

Preliminary Results

SUM over Q^2, Φ

OLD RPR

RPR-2011

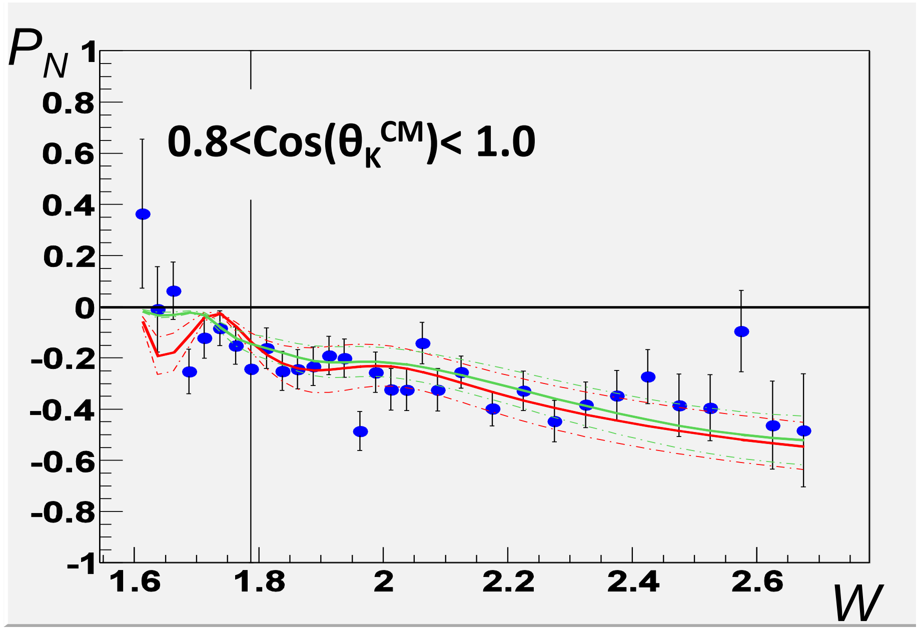

Induced Polarization P_N vs W (GeV)

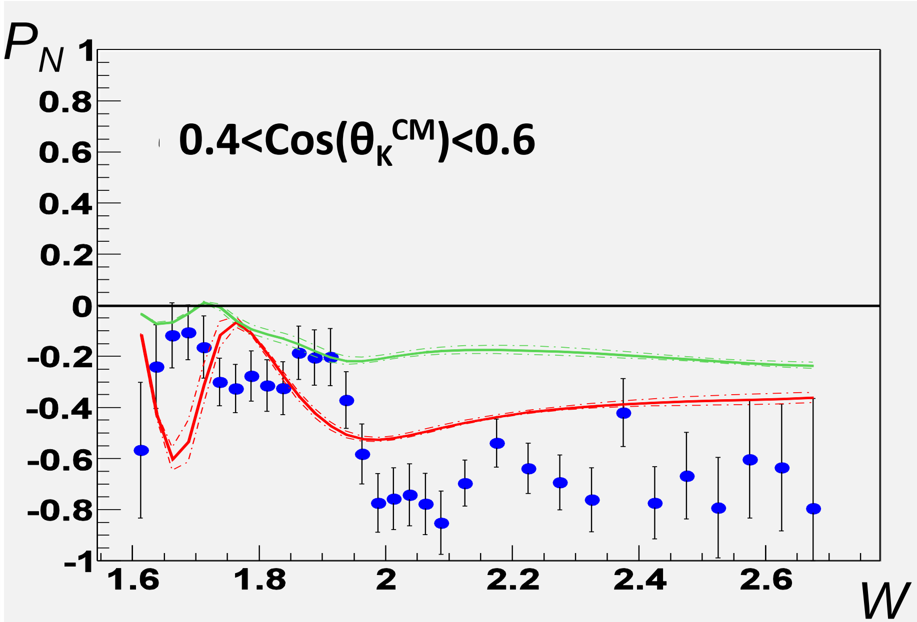

Preliminary Results

SUM over Q^2, Φ

OLD RPR

RPR-2011

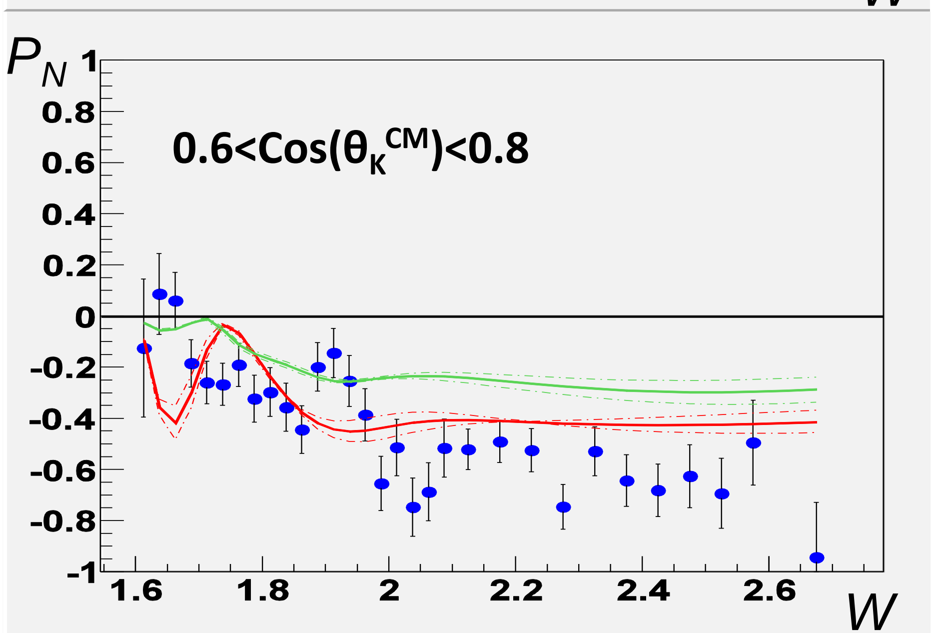

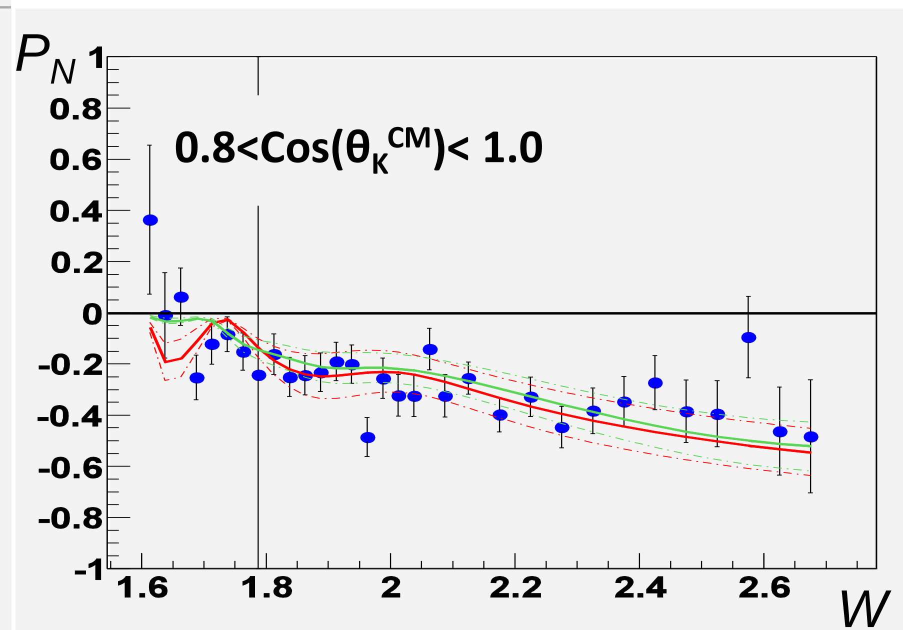

Induced Polarization P_N vs W (GeV)

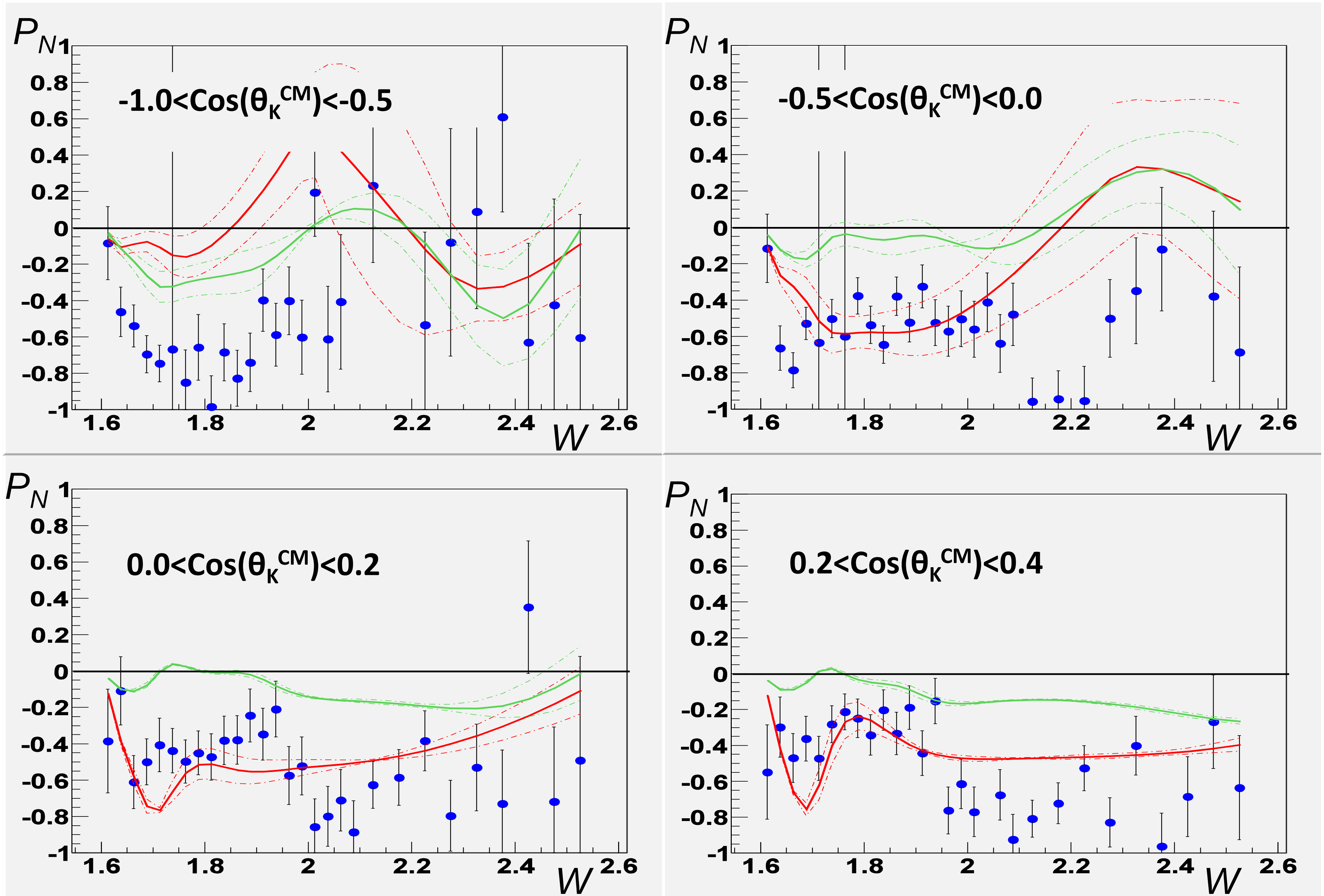

Induced Polarization vs. *W (photoproduction)*

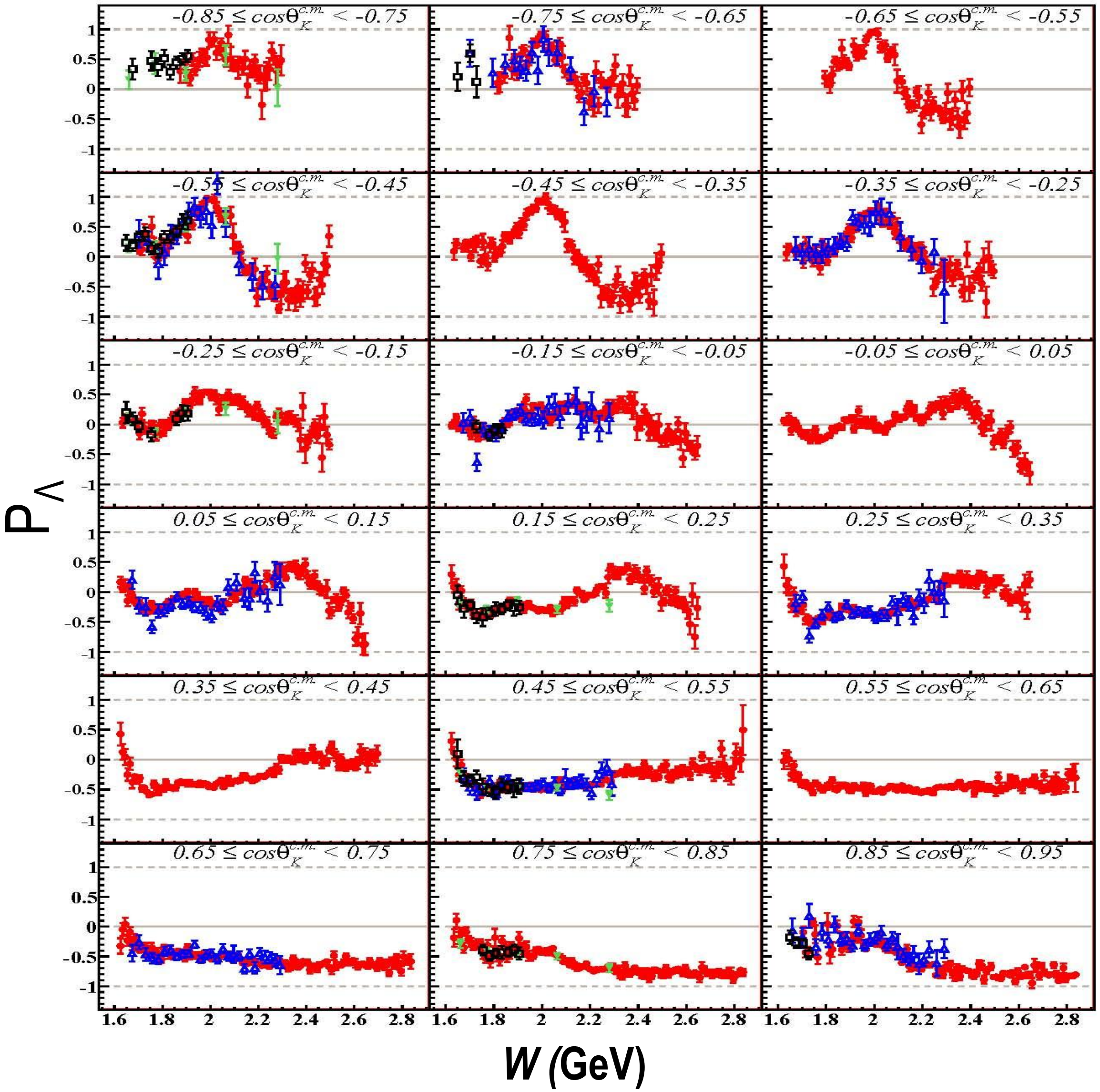

Red: McCracken, CLAS 2010
Blue: McNabb, CLAS 2004
Green: Glander, SAPHIR 2004
Black: Lleres, GRAAL 2007

Dashed lines indicate the physical limits of polarization.

M.E. McCracken *et al.*, Phys. Rev. C **81**, 025201 (2010).

Induced Polarization vs. *W (photoproduction)*

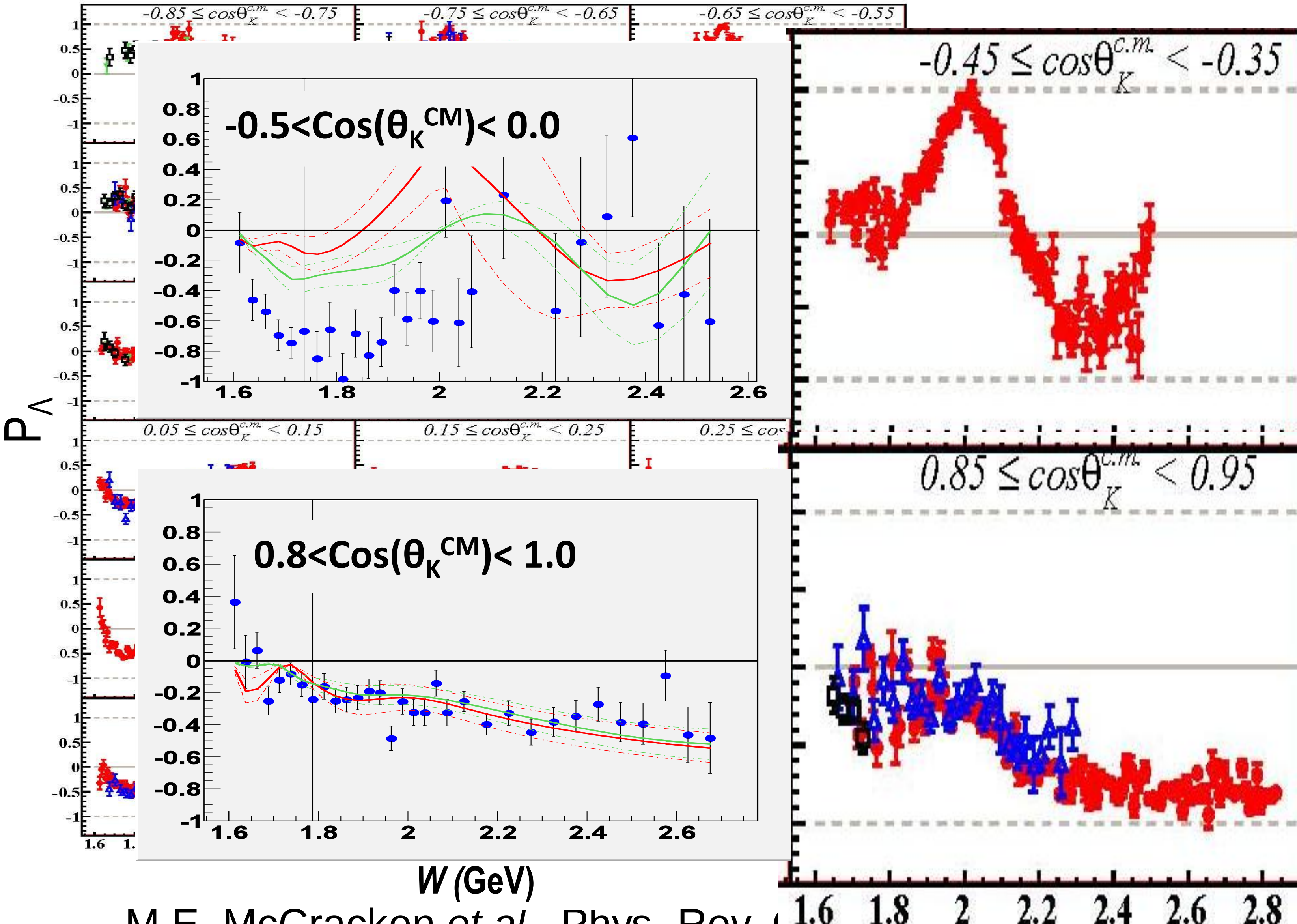

S 2010
2004
HIR 2004
2007

the
zation.

M.E. McCracken *et al.*, Phys. Rev.

SUMMARY

- Results show some features that are consistent with *s*-channel resonance contributions.

- Old RPR theoretical model calculations are in good agreement with experimental data at very forward kaon angles but they fail to reproduce the data at all other kaon angle bins.
    - RPR gives a reasonable description of photoproduction data (both for cross sections and polarizations at cos $\theta_K^{CM} > 0$).

- RPR-2011 reproduces overall magnitude of polarization, but fails to reproduce the structure, particularly around W=1.9 GeV.

SUMMARY (continued)

➢ Experimental data are similar for both electro- and photoproduction at forward kaon angles, but are very different for backward kaon angles.

➢ Unlike for photoproduction, no sharp change of sign is observed in electroproduction polarization data. This suggests that even small longitudinal polarization of the virtual photon in the interference terms may play a significant role in the production process.

NEXT…

- Comparison to different theoretical models is required to interpret our results.

Funded in part by: The U.S. Dept. of Energy, FIU Graduate School

Hadron Identification: Timing Method

$$\beta = \frac{p}{E} = \frac{p}{\sqrt{m^2 + p^2}}$$

$$m = \frac{p}{v} = \frac{p}{\left(\frac{\Delta x}{t_{TOF}}\right)} = \frac{p}{\Delta x} t_{TOF}$$

$$\delta t_\pi = t_{TOF} - t_\pi = t_{TOF} - \frac{m_\pi \Delta x}{p}$$

$$\delta t_K = t_{TOF} - t_K = t_{TOF} - \frac{m_K \Delta x}{p}$$

$$\delta t_p = t_{TOF} - t_p = t_{TOF} - \frac{m_p \Delta x}{p}$$

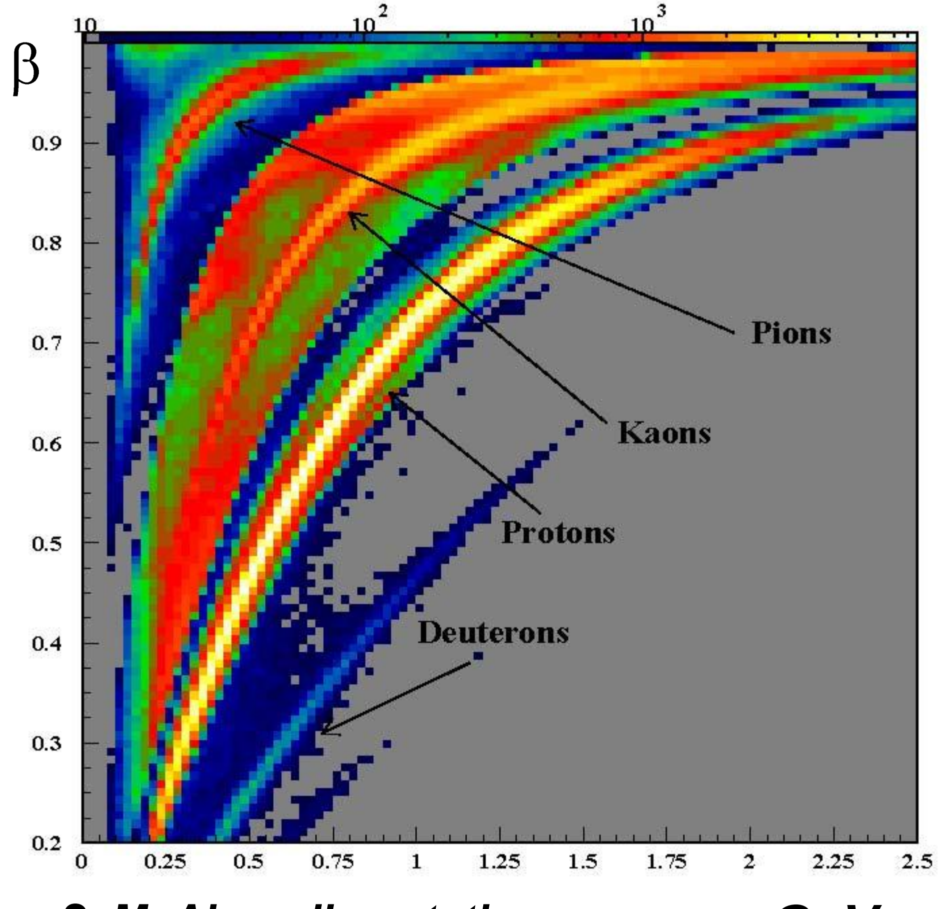

S. McAleer dissertation

The assumed mass that minimizes δt is assigned to the hadron.

Background Subtraction

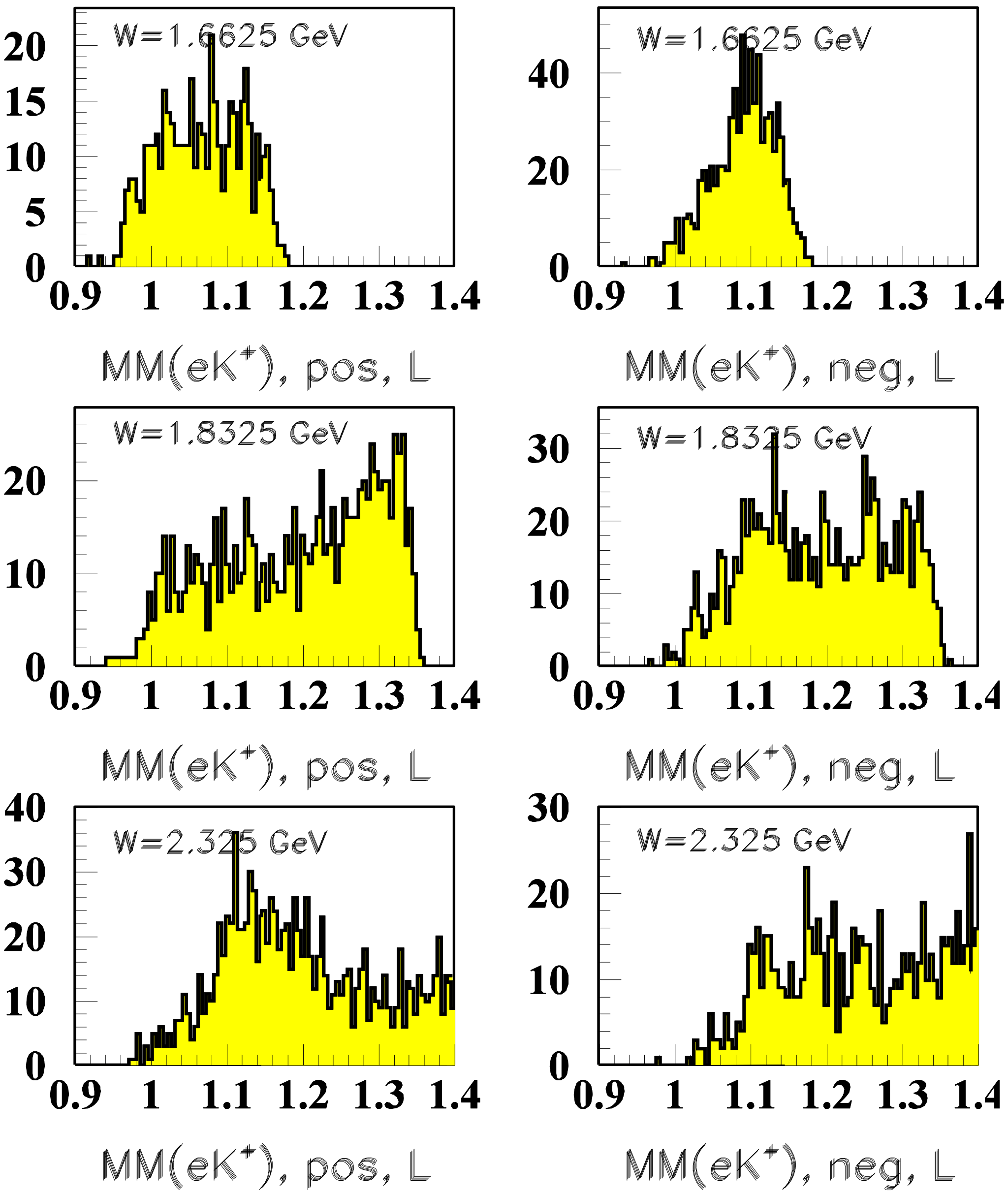

The background templates are generated from data by intentionally misidentifying pions as kaons.

f_{BKG}= A*(bkg_temp)

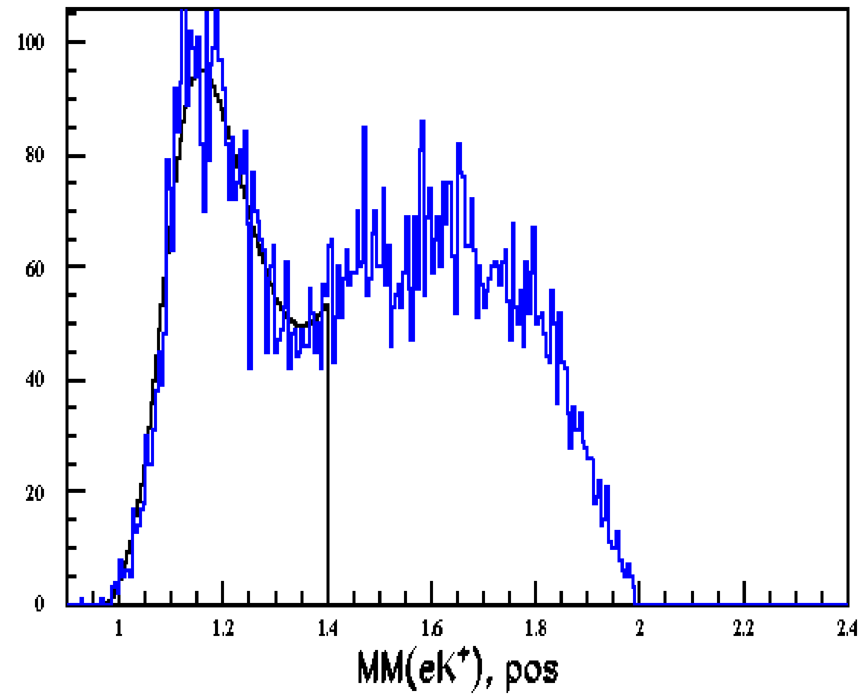

Background Subtraction

Reduced χ^2 Distributions

$0.6<\cos(\theta_K^{CM})<0.8$

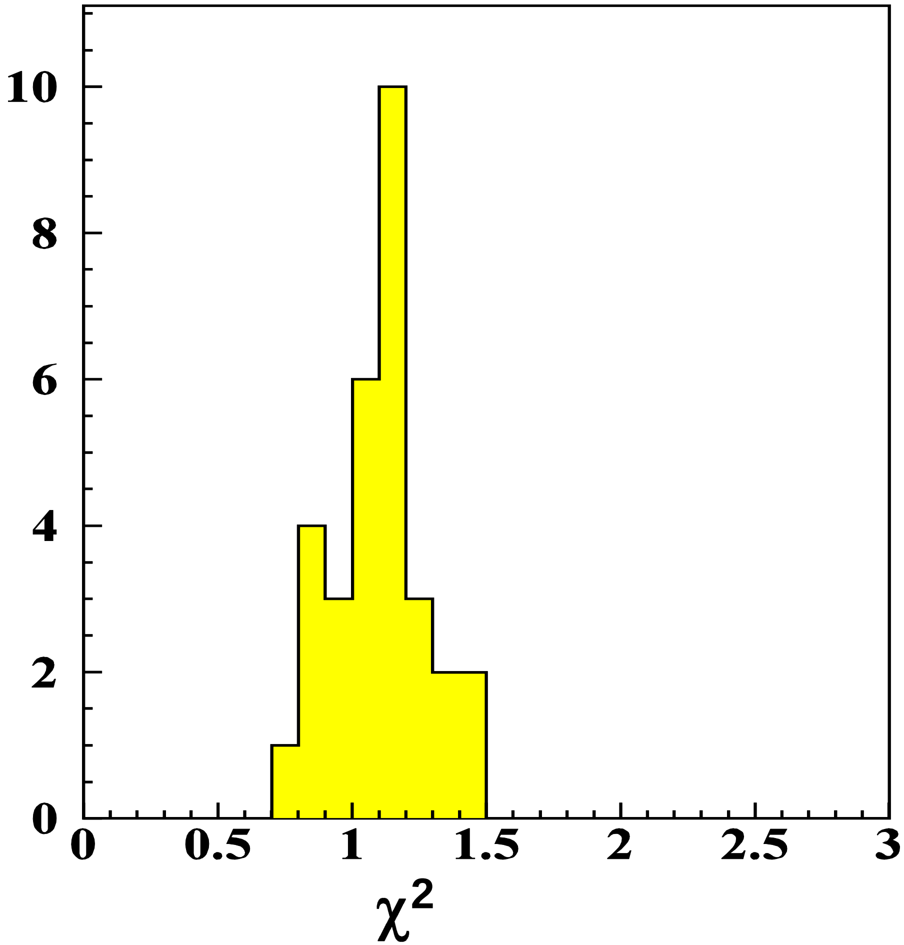

$0.8<\cos(\theta_K^{CM})< 1.0$

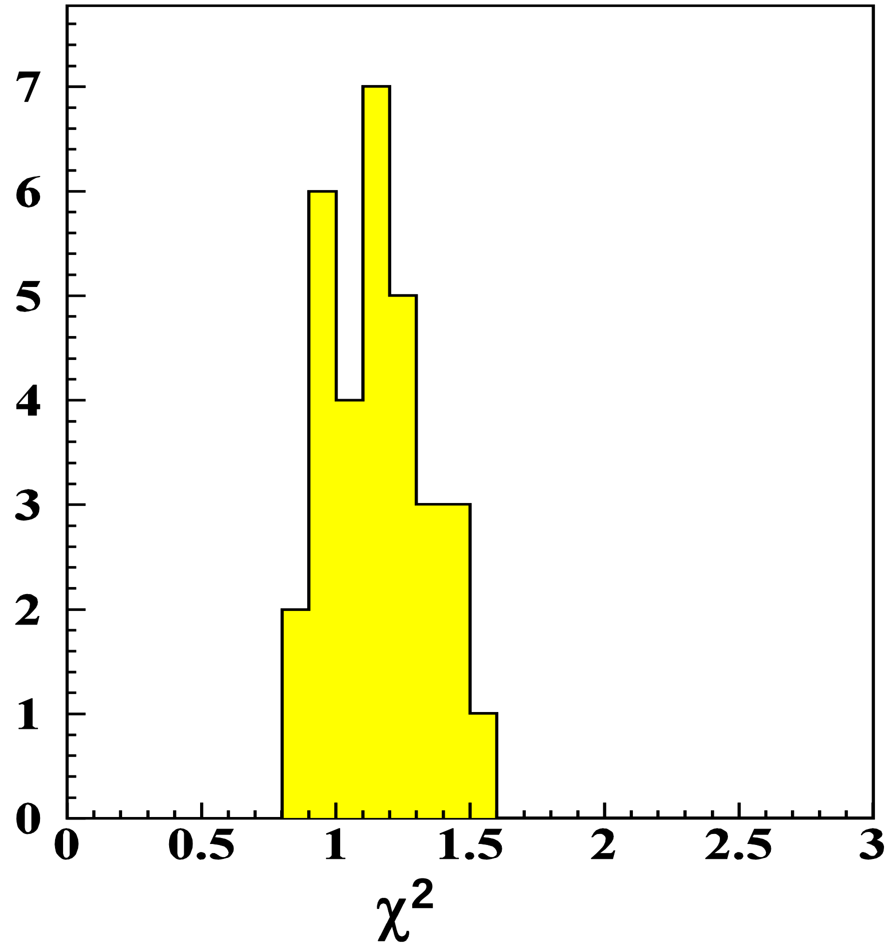

P_N vs. Q^2 dependence

$0.8 < \cos(\theta_K^{CM}) < 1.0$

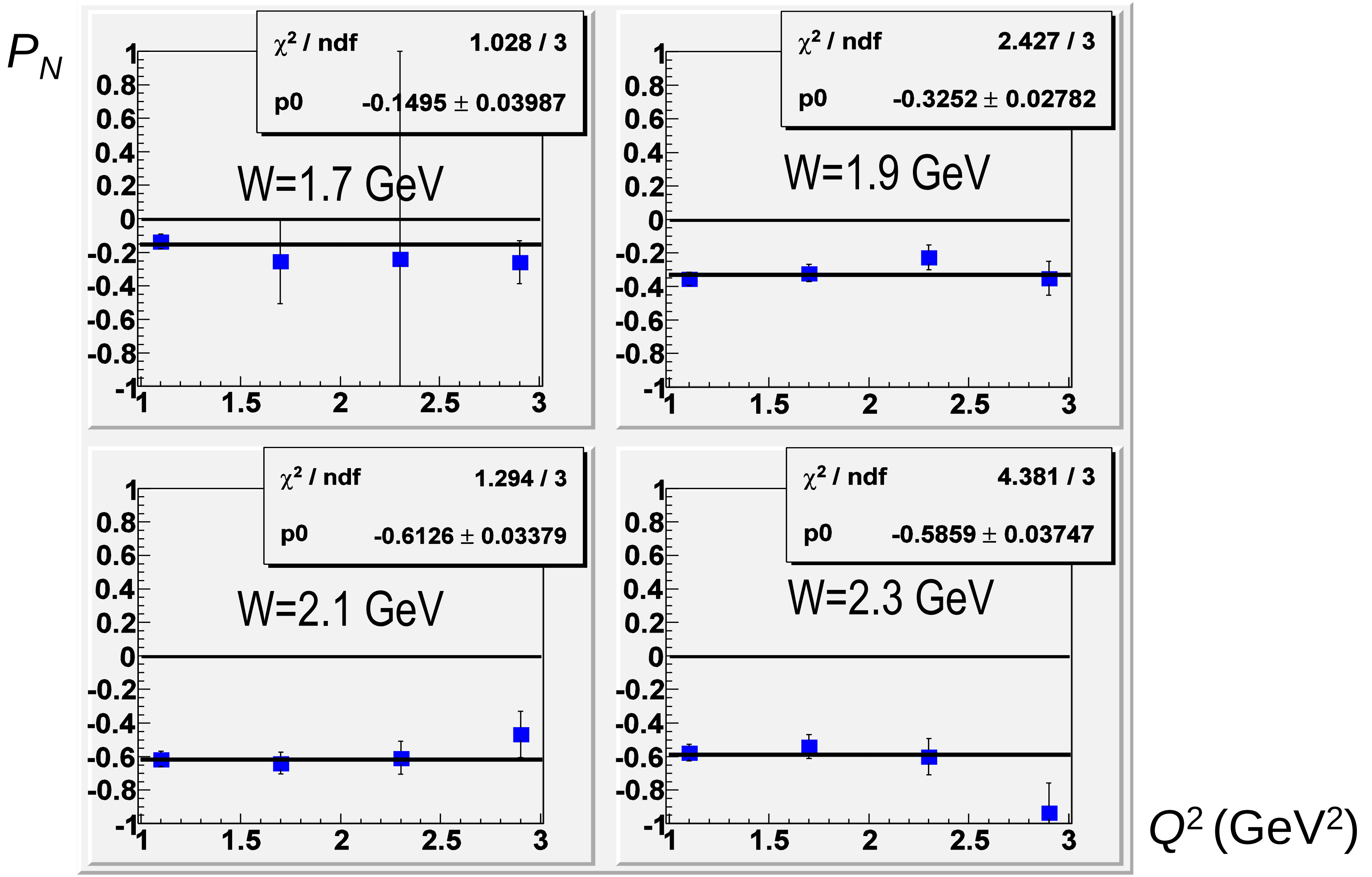

RPR-2011 Fits to Photoproduction Data

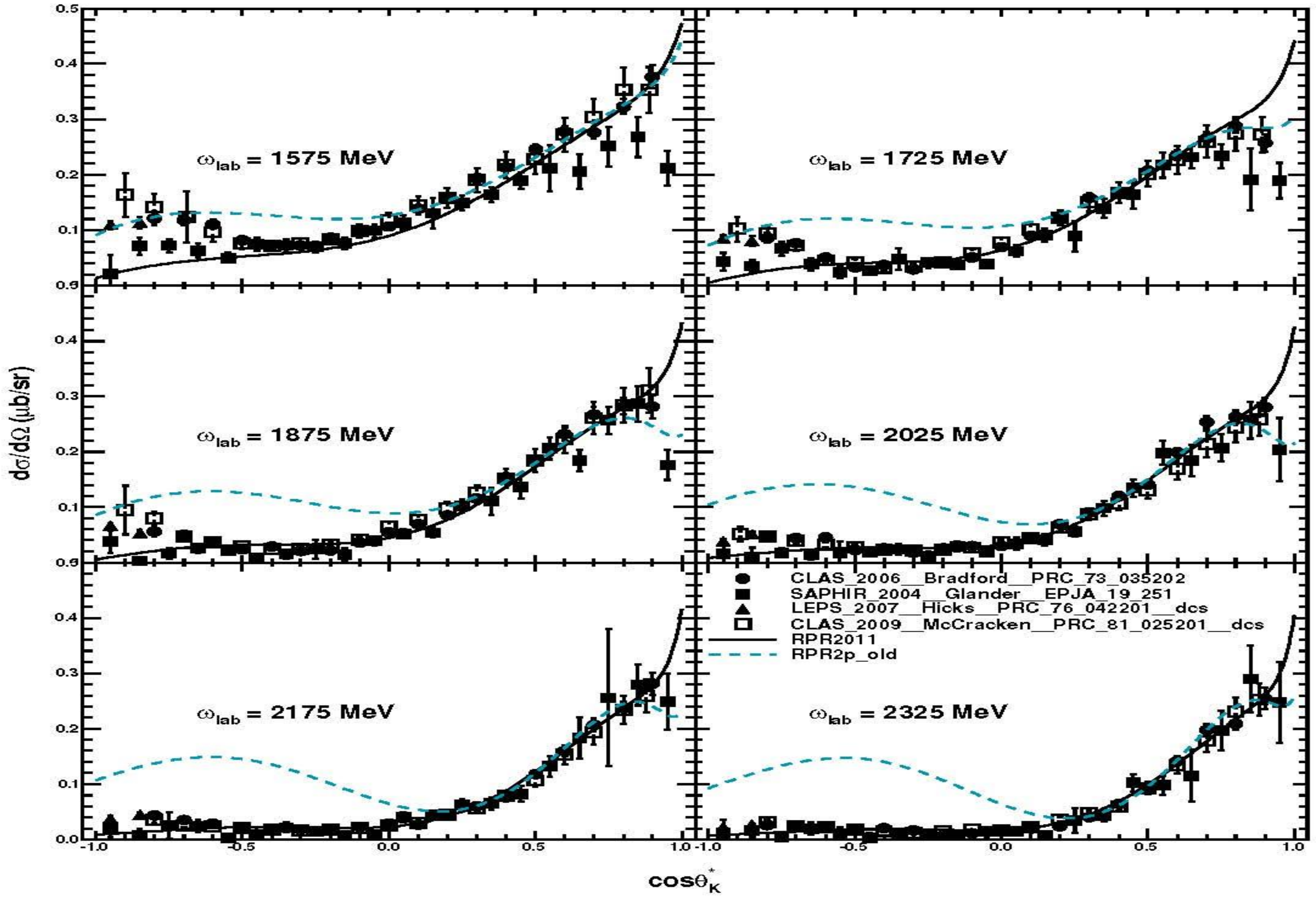

Induced Polarization P_N vs. $\cos(\theta_K^{CM})$

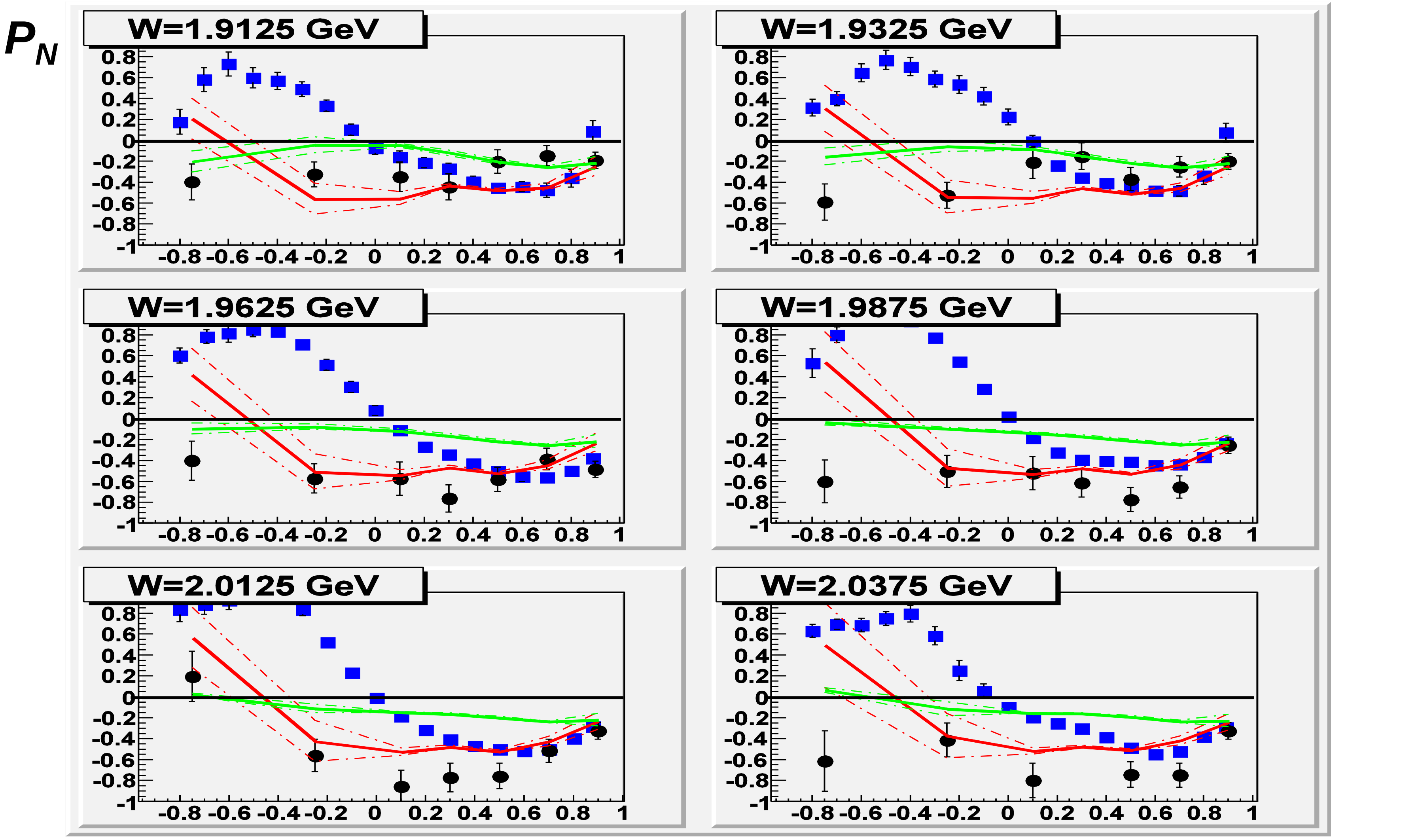

Blue: M.E. McCracken *et al.*, Phys. Rev. C 81, 025201 (2010).

Old RPR: T. Corthals *et al.*, Phys. Lett. B 656 (2007)

RPR2011: T. Vrancx *et al.*, arXiv:1105.2688

Systematic Uncertainties

Sources

- Polarization Extraction
- Acceptance
- Background Subtraction

Systematic uncertainty estimated as uncertainty-weighted average polarization.

$$\delta P = \sqrt{\frac{\sum_{i=1}^{n} \frac{[P_i^{nom} - P_i^{alt}]^2}{(\delta P_i^{nom})^2}}{\sum_{i=1}^{n} \frac{1}{(\delta P_i^{nom})^2}}}$$

Total systematic uncertainty in each $\cos(\theta_K^{CM})$ bin is the SUM of the uncertainties in quadrature from all sources. Sources are assumed to be uncorrelated.

Systematic Uncertainties: MM(eK^+) cut

Nominal: $1.05 < MM(eK^+) < 1.15$ GeV

Alternative 1: $1.025 < MM(eK^+) < 1.17$ GeV

Alternative 2: No Λ missing mass cut is applied

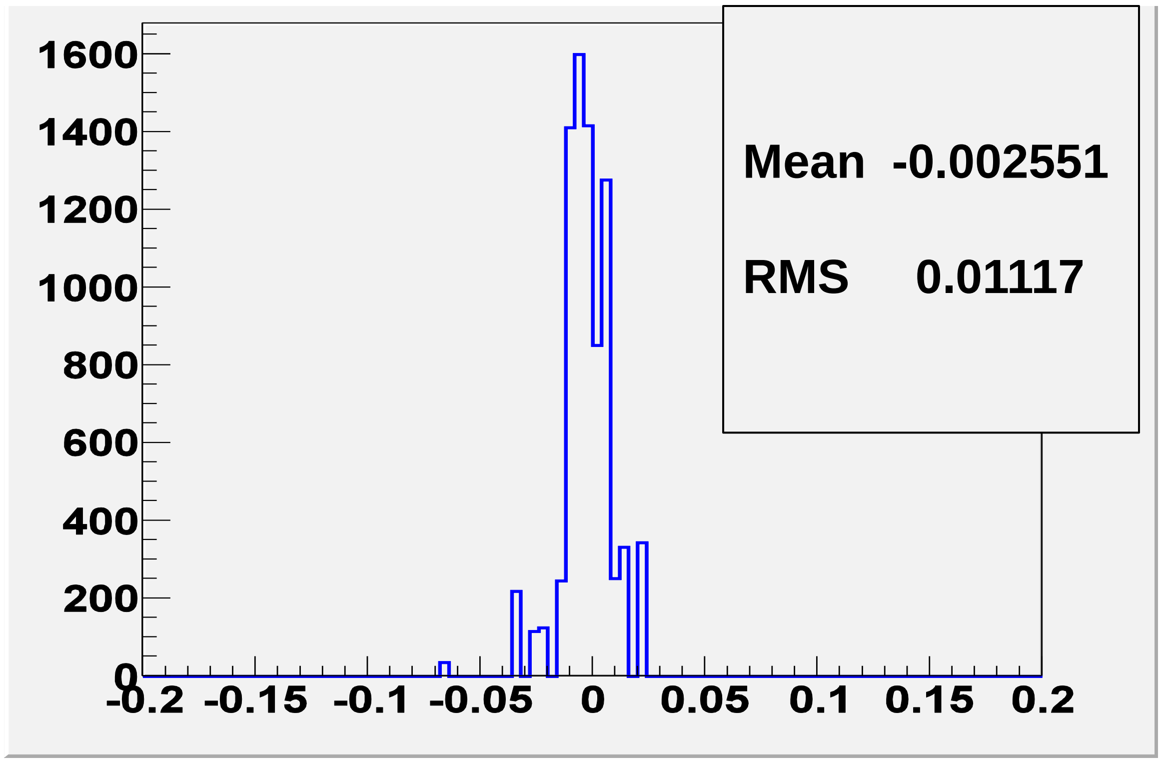

RMS of the uncertainty-weighted $\Delta P = P^{NOM} - P^{ALT}$ histogram is assigned as measure of systematic uncertainty from this source.

Systematics: Weighted RMS of $\Delta P = P^{NOM} - P^{ALT}$

Source \ $\cos(\vartheta_K^{CM})$	(-1.0,-0.5)	(-0.5,0.0)	(0.0,0.2)	(0.2,0.4)	(0.4,0.6)	(0.6,0.8)	(0.8,1.0)
Acceptance Corrections	0.011	0.026	0.014	0.013	0.012	0.013	0.011
MM(eK^+p)	0.042	0.025	0.047	0.036	0.046	0.041	0.033
Geometrical Fiducial Cuts	0.058	0.080	0.080	0.065	0.070	0.048	0.040
p Acceptance Corrections with polarized MC	0.086	0.064	0.080	0.085	0.080	0.093	0.075
Fit Method	0.046	0.052	0.044	0.034	0.031	0.030	0.031
Fixed /Float Fit Parameters	0.032	0.027	0.034	0.023	0.013	0.012	0.015
α	0.013	0.013	0.013	0.013	0.013	0.013	0.013
TOTAL	**0.126**	**0.124**	**0.136**	**0.121**	**0.122**	**0.118**	**0.099**

Cross Check of Systematics

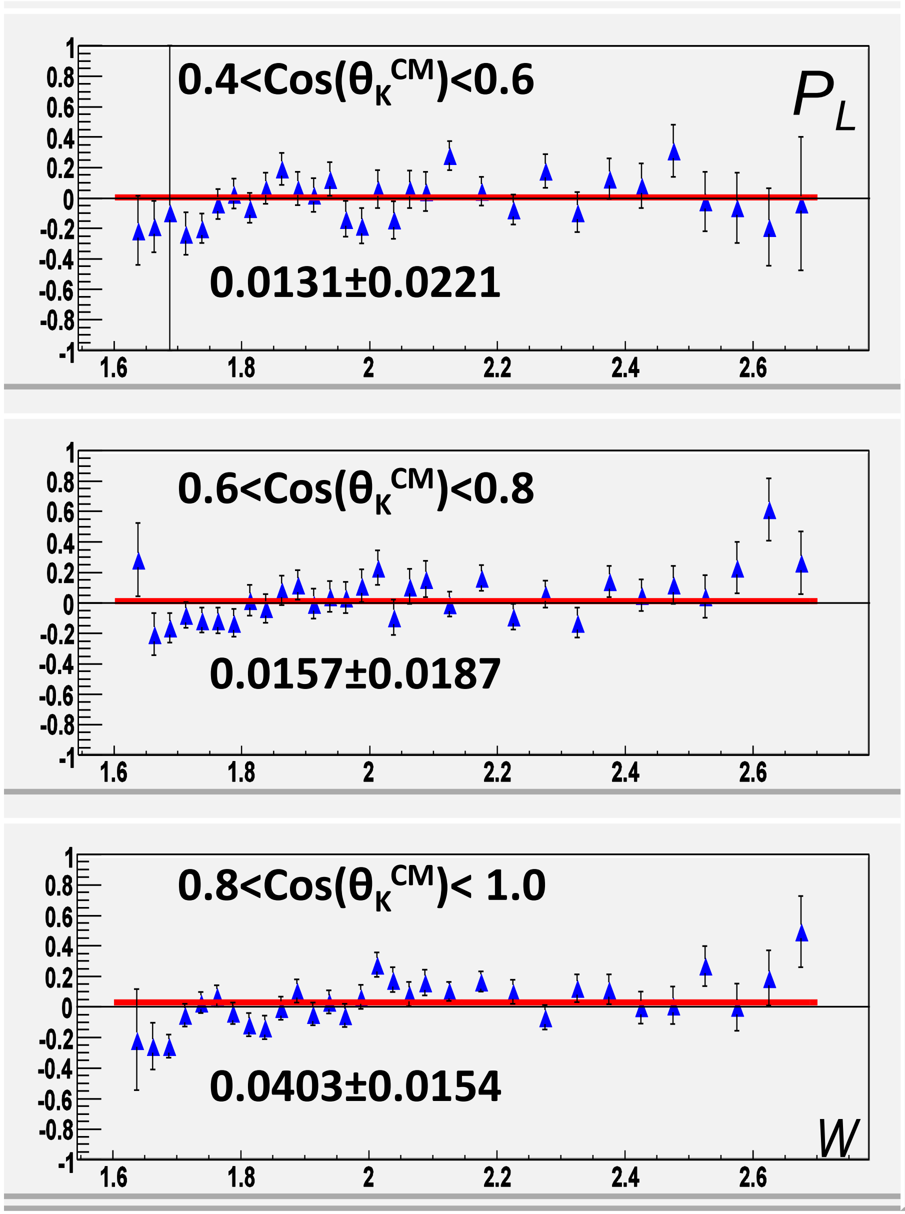

P_L and P_T deviations from 0 are consistent with table within uncertainties.